Engineering Structures 293 (2023) 116657

Contents lists available at ScienceDirect

Engineering Structures

journal homepage: www.elsevier.com/locate/engstruct

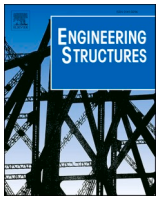

# Metamodel-assisted meta-heuristic design optimization of reinforced concrete frame structures considering soil-structure interaction

Iván Negrin [a,*], Moacir Kripka [b], Víctor Yepes [a]

[a] Institute of Concrete Science and Technology (ICITECH), Universitat Politècnica de València, 46022 Valencia, Spain
[b] Graduate Program in Civil and Environmental Engineering, University of Passo Fundo, Km 292, BR 285, Passo Fundo 99052-900, RS, Brazil

ARTICLE INFO

*Keywords:*
Structural optimization
Reinforced concrete
Frame structures
$CO_2$ emissions
Metamodel
Kriging
Soil-structure interaction

ABSTRACT

It is well known that conventional heuristic optimization is the most common approach to deal with structural optimization problems. However, metamodel-assisted optimization has become a valuable strategy for decreasing computational consumption. This paper applies conventional heuristic and Kriging-based meta-heuristic optimization to minimize the $CO_2$ emissions of spatial reinforced concrete frame structures, considering an aspect usually ignored during modeling, such as the soil-structure interaction (SSI). Due to the particularities of the formulated problem, there are better strategies than simple Kriging-based optimization to solve it. Thus, a meta-heuristic strategy is proposed using a Kriging-based two-phase methodology and a local search algorithm. Three different models of structures are used in the study. Results show that including the SSI leads to different design results than those obtained using classical supports. The foundations, usually ignored in this type of research, also prove significant within the structural assembly. Additionally, using an appropriate coefficient of penalization, the meta-heuristic approach can find (on average) results up to 98.24% accuracy for cohesive soils and 98.10% for frictional ones compared with the results of the heuristic optimization, achieving computational savings of about 90%. Therefore, considering aspects such as the SSI, the proposed metamodeling strategy allows for dealing with high-complexity structural optimization problems.

## 1. Introduction

Design optimization is a topic widely discussed in the current context of structural design due to the need to minimize construction costs, material use, and decrease the construction sector's negative impact on the environment [1]. It can be achieved by strategies such as the use of novel building materials (e.g., low-carbon cement and clinker substitutes) [2] and recycling [3], but also through the more efficient use of these materials resulting from their design optimization [4].

As a result, more optimization objectives beyond economic ones have been emerging. A primary view of environmental assessment can be applied using single criteria reliably representing environmental impact. The most representative ones are $CO_2$ emissions and embodied energy (EE) [5], which have proven to hold a direct relationship with economic cost [6,7,8].

Structural optimization problems have two main ways to be solved. On the one hand, exact methods are generally based on mathematical programming. On the other hand, heuristics consist of artificial intelligence strategies that imitate natural processes [9]. These algorithms are excellent alternatives to solve large-scale and highly nonlinear optimization problems, as is usually the case with structural optimization [10], especially related to reinforced concrete (RC) structures optimization. For this reason, it is habitual to find structural optimization problems solved by heuristics. In the books proposed by Kaveh [11,12], many examples of optimization problems in the design of civil engineering structures (mainly skeletal ones) can be found. However, more than these simple procedures are required to deal with real-life challenging optimization problems. Alternatively, meta-heuristics have arisen to handle such problems. They blend several simple strategies intelligently to explore the solution space more efficiently.

Reinforced concrete (RC) frame building structures comprise a significant portion of the construction sector. They are associated with substantial economic costs and environmental impacts [13]. Therefore, it is crucial to obtain designs that minimize the adverse effects and maximize the advantages of this construction type. Several authors have carried out studies to optimize these structures. Most of these studies focus on essential concrete elements or two-dimensional frames. Only a few authors have applied design optimization to three-dimensional RC

* Corresponding author.
*E-mail address:* ianegdia@doctor.upv.es (I. Negrin).

https://doi.org/10.1016/j.engstruct.2023.116657
Received 15 March 2023; Received in revised form 18 July 2023; Accepted 23 July 2023
Available online 31 July 2023

frame buildings, including notable examples [14–18]. It is mainly due to the high complexity involved in modeling these structures. Therefore, high computational consumption is one of the most critical challenges in structural optimization problems. The solution for most of these engineering problems consists of accurate and expensive numerical methods, usually represented by partial differential or integral equations, e.g., structural finite element analysis (FEA), where a single function evaluation is usually considerably time-consuming [19]. Thus, if common optimization problems involve thousands of single-function evaluations, structural optimization problems generally require significant time and computational resources. Based on this, metamodel-assisted structural design optimization (MASDO) has arisen as a valuable alternative to deal with these complex problems. This kind of meta-heuristic approach uses a surrogate model instead of the complex one to perform the simulations of the optimization procedure. The most basic methodology consists of obtaining a group of design vectors inside the design space, for which high-fidelity simulations (e.g., FEA) are performed. Then, the high-fidelity values regression or interpolation models are built and can be analyzed by, e.g., optimization algorithms [19]. Applying this strategy with the combination of clever optimization methodologies can be very useful in quickly obtaining good optimization results. The most common metamodels are polynomial regression, Neural Networks (NN), and Kriging models [20]. However, Kriging methodologies have been one of the most used to aid structural optimization problems due to their simplicity and effectiveness. They create a metamodel using optimal interpolation based on regression against observed values of the surrounding data points, weighted according to spatial covariance values [5].

On the other hand, another problem usually found in the literature is the non-inclusion of modeling aspects such as the soil-structure interaction (SSI). Authors usually assume structures with idealized or classic supports (e.g., fixed), even when the assembly of soil and foundations is not perfectly rigid. Support displacements (settlements) exist and influence how the superstructure works, which is not the case with classic supports. This idealization (no SSI consideration) leads to an inefficient superstructure design. Due to the nature of settlement occurrence, it will suffer an accelerated deterioration with the consequent need for extra maintenance during its life cycle [21,22,23].

Moreover, several distinctions must be considered between static and dynamic SSI in the analysis being performed for the SSI consideration. An example of a dynamic SSI implementation can be found in [24], where foundations are modeled as rigid strip footings, and the soil is layered with constant material properties along its depth. An approach similar to the one used in [25] is considered to build the constitutive model of the soil, where the shear wave velocity and the friction angle are considered parameters of the soil layers. Otherwise, considering this study's static approach, SSI is considered to adopt a Winkler model, as proposed by [26]. Thus, to relate the contact soil pressure $p$ to the foundation settlement $S$, only one equation that includes both linear and non-linear soil behavior is considered. Therefore, in this work, instead of creating a three-dimensional model of the soil, the vertical direction is eliminated while considering the behavior in this direction by modeling the contact of the foundation and the soil as a discrete number of springs of stiffness $k$. This stiffness depends directly on $p$ and $S$.

Considering the SSI during modeling, this paper applies conventional heuristic optimization and a Kriging-based meta-heuristic optimization strategy to optimize spatial RC frame structures. For this reason, the two main goals are to demonstrate the differences in optimizing the design of a structure with idealized supports and considering the SSI using two types of soils. Secondly, to implement a Kriging-based structural optimization strategy to reduce the high computational consumption of the conventional heuristic optimization trying to keep accurate optimization results. Consequently, the organization of the paper is as follows. Section 2 explains the general methodology, including the problem description, the explanation of the SSI consideration, the formulation of the optimization problem, and the strategies used to solve it. Section 3 is dedicated to exposing and discussing the results. Finally, conclusions are drawn in Section 4.

## 2. Methodology

### 2.1. Problem description

In this paper, the structure used in previous work [8] is implemented as the basis of the investigation. Additionally, two other case studies similar to the basic one are used to generalize the results. In these, the span lengths (CS-2) and the number of levels (CS-3) are varied (see Fig. 1). The cross-sections of the elements are rectangular. This research's novelty lies in including shallow foundations and the corresponding SSI during modeling. Note that the shallow individual footing variant is selected as it is the one that would best suit the modeled structures. If the height of the structures is increased, there will come a time when the base area of the foundations will be so large that they will overlap. It is where other typologies, such as combined footing or mat foundations, would be necessary. If the height of the building continues to increase, the use of piles would be required to increase the bearing capacity of the foundations, which opens the possibility of using the mat-pile combination. On the other hand, using the simpler typology allows better applicability of the proposed methodology, which, once validated, can be applied to other more complex structures.

The loads imposed on the system are shown in Table 1. Eqs. [1–4] define the essential load combinations used, where D, L, and W are the dead, live, and extreme wind loads, respectively. It is essential to highlight that other combinations are used to design the foundations and to check the serviceability limit state.

$$1.2D + 1.6L \tag{1}$$

$$1.2D + 0.8W \tag{2}$$

$$1.2D + 1.4W + 0.5L \tag{3}$$

$$0.9D + 1.4W \tag{4}$$

Some features are considered in this problem to obtain relevant results from a practical structural engineering point of view. The variables are discrete to handle with constructive dimensioning of the elements and real types of concrete. Additionally, solutions of reinforcement (longitudinal and transversal) are adapted to commercially available bar diameters, including longitudinal bars cut-off (detailing) and their actual placement in the cross-sections of the elements (see Fig. 2).

Other aspects generally ignored by designers, such as the reduction of elements' stiffness by cracking, second-order analysis of structures, and the after-mentioned SSI consideration, are also included. The CSiSAP2000 platform is used as a calculation engine via the Applied Program Interface (API) SAP2000-MATLAB to deal with such a problem. For the creation of the models, the superstructure elements are considered frame type. The foundations are modeled as shell elements. They are discretized (meshed) to improve their behavior as slab footings. A sensitivity analysis concluded that four divisions in each direction are sufficient for good results. Now, these elements are initially loose. It is where the soil-structure interaction comes in. To simulate this phenomenon, a stiffness coefficient k is calculated (see section 2.2), which can be assigned in two ways: as an area (directly to the bottom surface of the element) or distributed to the nodes formed by discretizing the element. In this case, the first way is used because it is faster from the computational point of view. In either case, the results are the same. A complete structure model can be seen in Fig. 3(a). The frame structure design for strength and serviceability Limit States is based on the ACI 318–14 code.

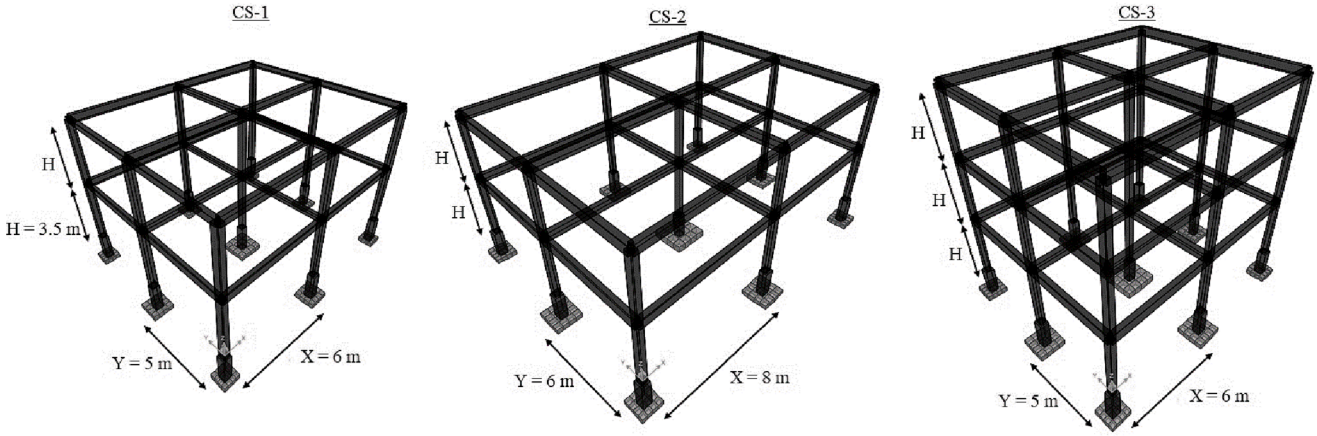


**Fig. 1.** Three case studies (CS). CS-1 is the basic case study, CS-2 is similar to CS-1, but X and Y are 8 and 6 m respectively, and CS-3 is CS-1 with an additional level.

**Table 1**
Loads considered.

| Description | Value |
|---|---|
| Dead load on first floor | 4.80 kN/m$^2$ |
| Dead load on roof | 5.43 kN/m$^2$ |
| Live load on first floor | 4.00 kN/m$^2$ |
| Live load on roof | 0.80 kN/m$^2$ |
| Wind load | 0.92 kN/m$^2$ 0–5 m, 1.01 kN/m$^2$ at 7 m, 1.13 kN/m$^2$ at 10.5 m. |

### 2.2. Implementation of the static soil-structure interaction

When considering the static SSI in the structural optimization problem, it is assumed that the structure above the underlying soil deforms under loading–unloading, which results in a redistribution of internal forces in the superstructure. The soil is modeled as a linearly elastic half-space, considering the depth constraint of compressible thickness, while the foundation is considered a shallow slab footing (see Fig. 3(a)).

In practical calculations, the consideration of non-linearity in determining settlements in type II collapsible soils was introduced in [26]. However, this model can be adapted and extended to other soil types and foundation typologies [27]. In his 1969 study [26], Klepikov introduced an approximation of the relationship between acting pressure and settlement ($p$ vs. $S$) for a shallow foundation on a soil base. He represented this relationship through a hyperbolic equation, denoted as Eq. (5). The "pressure-settlement" curve passes through the point with coordinates ($\acute{R}^*$,$\overline{S}$) and unlimitedly approaches the asymptote $p$=$q^*_{br\_II}$ (see Fig. 4(a)).

$$S = \frac{p \cdot \overline{S} \cdot \left( \left( \frac{q^*_{br\_II}}{\acute{R}^*} \right) - 1 \right)}{q^*_{br\_II} - p} \tag{5}$$

Here, $\overline{S}$ is the base settlement for an acting pressure equal to the soil base linearity limit stress $\acute{R}^*$ and $q^*_{br\_II}$ is the base bearing capacity pressure, based on expressions from the theory of plasticity. On the other hand, the soil base "secant" stiffness coefficient $k$ can be obtained easily for the loading stage as in Eq. (6) [27].

$$k = \tan\alpha = \frac{p}{S} = \frac{q^*_{br\_II} - p}{\overline{S} \cdot \left[ \left( \frac{q^*_{br\_II}}{\acute{R}^*} \right) - 1 \right]} \tag{6}$$

This stiffness coefficient is applied to the finite springs introduced in the nodes created when meshing the foundation base. By making more divisions, the foundation will have a more realistic behavior, but the model will become more complex. Fig. 3(b) shows how the elements are discretized. On the other hand, Fig. 3(c) shows the non-uniform pressure distribution for an exterior foundation. It is because the foundations settle irregularly, depending on the loads coming from the superstructure, i.e., the springs deform according to their stiffness $k$ depending on the configuration of the superstructure and the foundation itself. This model has the limitation that the springs have a linear behavior. However, when applied superficially to the base of the foundation, the nodes formed when discretizing the element will have a coefficient according to their position in the element (interior, exterior, and corner). In addition, these nodes will deform according to the load each receives,

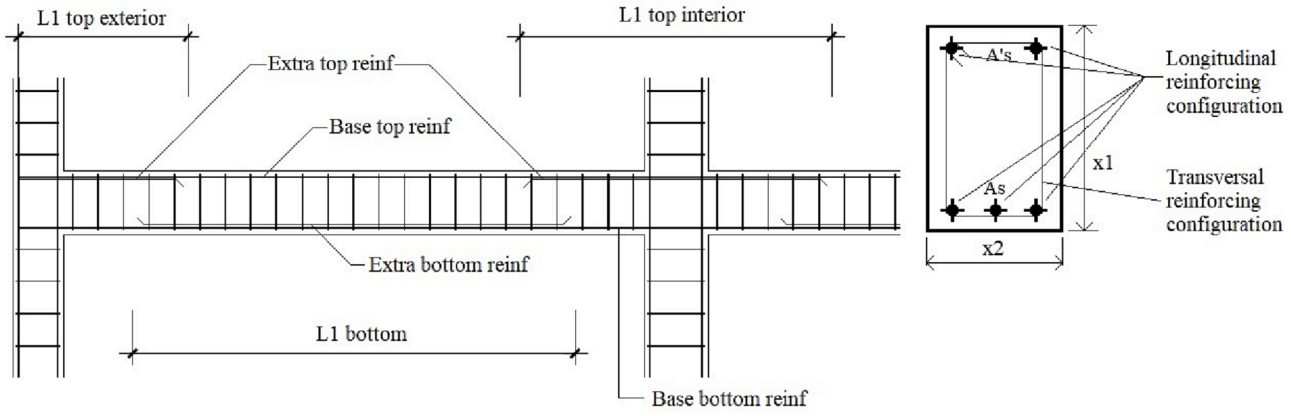


**Fig. 2.** Transversal and longitudinal reinforcement bars cut-off and distribution in RC building frames, x1 and x2 are design variables, As y A's are the real steel area in traction and compression respectively [1].

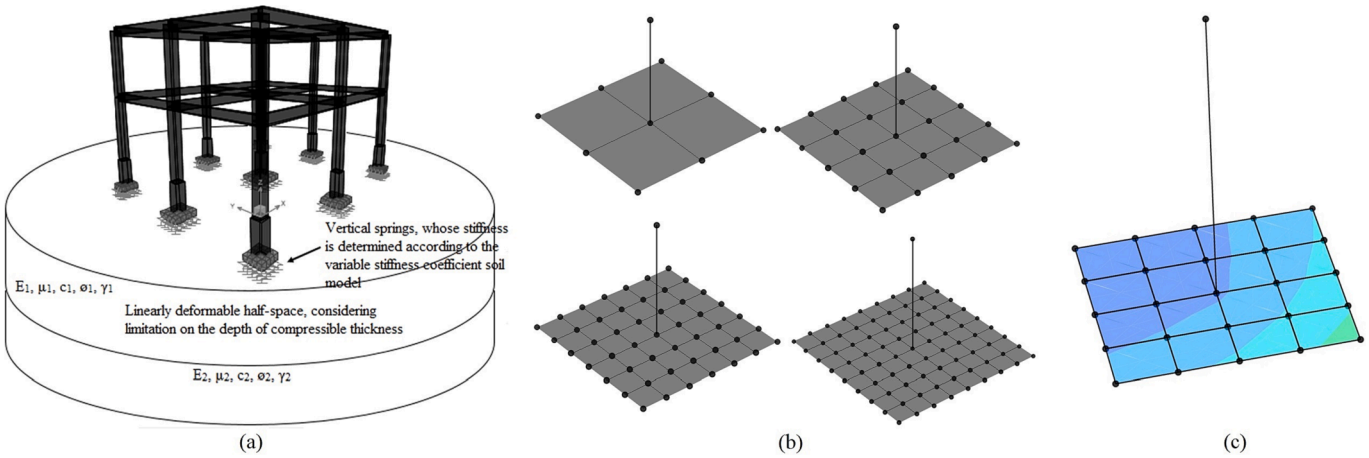


**Fig. 3.** Concepts related to SSI modeling: (a) general considerations, (b) meshing of shell elements, and (c) non-uniform pressure distribution of a foundation base.

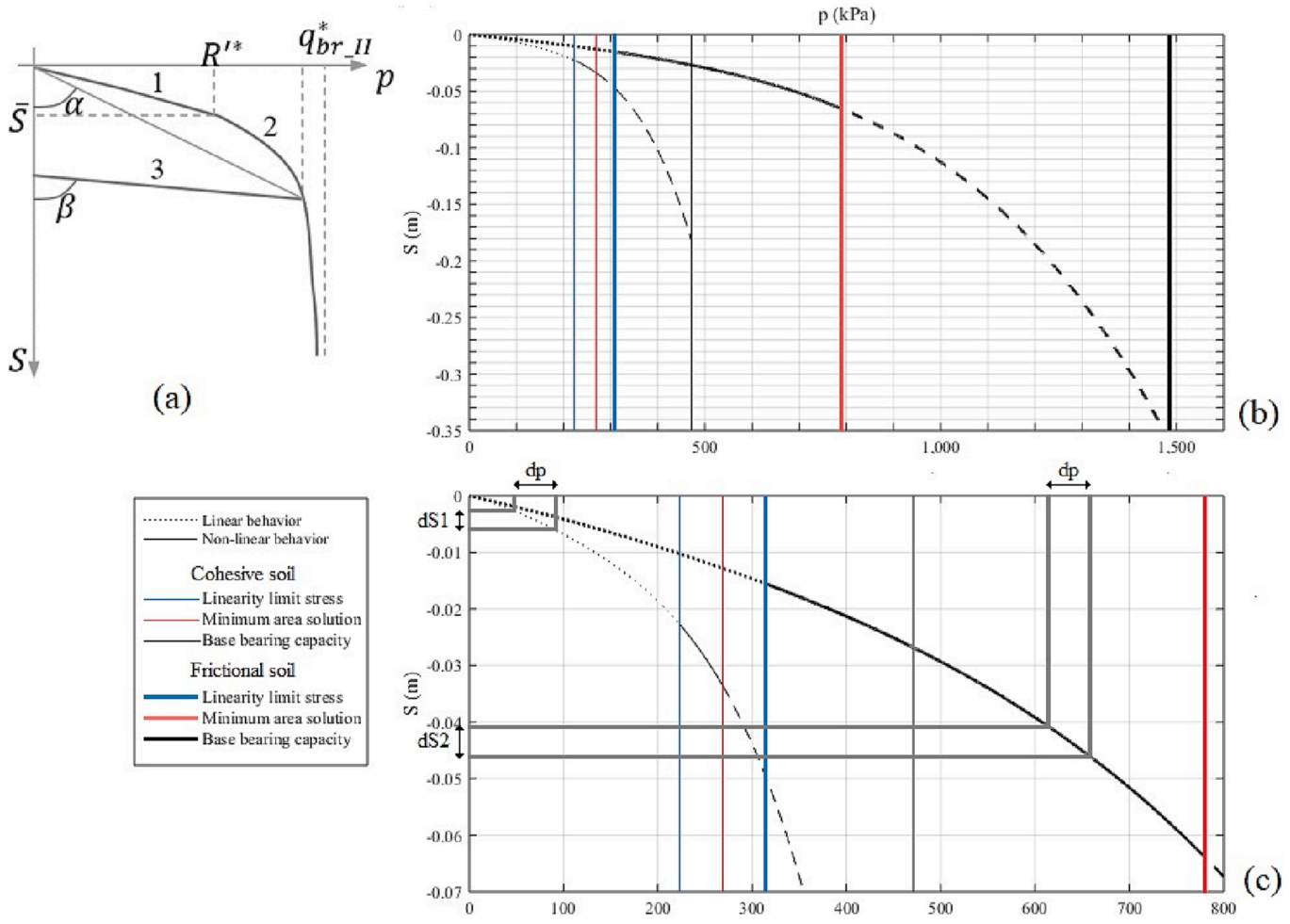


**Fig. 4.** Curve representing the acting pressure and settlement (p vs. S), (a) is an abstraction, (b) is the real p vs. S curves for an interior foundation and (c) is a zoom of the graphic of (b). Here, Ŕ* is the linearity limit stress, $\bar{S}$ is the base settlement for an acting pressure equal to the soil base linearity limit stress Ŕ* and q*br_II is the base bearing capacity pressure. For more information, refer to [1].

distributed non-uniformly throughout the shell element. Thus, the nodes formed (1) have different coefficients, and (2) receive different loads. Therefore, the foundation can not only settle but also rotate. Thus, the behavior of the supports is very much in line with what happens in reality. It is obviously not the case with rigid supports. It is important to note that several authors have validated this strategy of relating pressure and settlement. According to [28], this curve is acceptable for obtaining soil stiffness when considering SSI. It has been proven in actual experiments for different soil types [29,30,31,32].

It should be noted that the model proposed for considering the SSI is relatively simple. Even so, and taking into account that it is based fundamentally on the calculation of the actual settlements S, several

aspects could be indirectly considered, such as: inhomogeneity of the geological structure of the base, presence of water level, separate soil lenses and different inclusions, the possibility of soil flooding and change of its properties, particular consideration of residual and elastic settlements of the base, and more. If future research would like to include any of these aspects, providing more information about these special soil conditions underlying the foundations would be beneficial. A highly detailed explanation of the considerations for modeling SSI can be found in [1].

#### 2.2.1. Pressure-settlement curves for different type of soils

One of the points to highlight in this study is the inclusion of the SSI during modeling and its influence on the structure's optimal design. Another aspect being considered is the underlying soil's influence. For this purpose, two soils are used in the SSI modeling. Soil 1, as seen in Table 2, is predominantly cohesive, while soil 2 is predominantly frictional.

It is essential to analyze how the soils behave during loading to understand how the superstructure performs based on the soil type. It is achieved by using actual behavior curves of the soils for a specific type of foundation. These curves are similar to the one depicted in Fig. 4(a), which is an abstract representation. The theory behind this approach is that differential settlements result in a redistribution of the internal forces of the superstructure, causing an increase, particularly in the bending moment.

Fig. 4(b) displays the curves for an interior foundation, where the thick line represents soil 2, and the thin one represents soil 1. It is observed that soil 2 has a greater bearing capacity than soil 1 and exhibits a larger zone of non-linear behavior, unlike soil 1, where the zone of non-linearity is minimal. It causes that underneath the foundation, type 1 soils generally present a linear behavior, while type 2 soils behave non-linearly. Therefore, differential settlements are more significant in type 2 soils. In Fig. 4(c), the curves are zoomed in. Suppose that dp is the possible difference in pressures of two adjacent foundations, e.g., an interior one with more pressure than an exterior one. This difference dp is placed in the usual working zone for each soil type, which is not precisely at the bearing capacity limit $q^*_{br\_II}$ (continuous black vertical line in Fig. 4(b)) but shifted to the left. The curve is a function of the settlement S and is constructed for Limit State II. At the same time, the geotechnical design of the foundation is made according to Limit State I, with different safety coefficients. Thus, the real points of p vs. S are moved. Therefore, while in soil 2, this movement keeps the points in a zone of non-linearity, in soil 1, they move to the area of linear behavior. The zoomed graph shows how the same difference in pressure dp causes a larger difference dS in soil 2 (with non-linear behavior) than in soil 1 (with linear behavior). Therefore, it can be said that this type of structure behaves more irregularly on type 2 soils than on type 1 soils.

#### 2.2.2. Algorithm for SSI modelling during structural optimization

For the SSI consideration, it is necessary to start from some point. Accordingly, the calculation starts by analyzing a model with idealized supports (fixed for this case). Based on the results of the first step, the geotechnical design is performed. Here, the dimensions of the foundations are calculated, and the structural design is also performed. Then, the stiffness coefficient is calculated for each group of foundations. This step is called the pre-design of the foundation. With these results, the previous model is completed with the foundations and the springs with k stiffness. The model analysis with the SSI consideration is carried out next, leading to new values of internal forces. The final design of the whole structure is performed. Then, the $CO_2$ emissions are obtained according to the total volume of work. Fig. 5 represents this process.

**Table 2**
Properties of the soils considered in the study.

| Soil | FI | C | E | γ | μ | ø |
|---|---|---|---|---|---|---|
| | (°) | (kPa) | (MPa) | kN/m$^3$ | | (°) |
| 1 | 8 | 60 | 12 | 19.0 | 0.40 | 76 |
| 2 | 32 | 10 | 15 | 17.5 | 0.30 | 56 |

FI: Soil friction angle C: Cohesion E: Modulus of elasticity γ: Density μ: Poisson's ratio
ø: see Fig. 6

### 2.3. Formulation of the optimization problem

The economic cost is probably the most widely implemented objective in optimizing the design of reinforced concrete structures. However, the environmental approach to optimization problems has arisen in recent years. The environmental impact of buildings can be directly measured using simple targets such as EE or $CO_2$ emissions.

Several studies have established comparisons between optimizing using economic or environmental criteria. In [33], it is compared the results of optimizing the economic cost and $CO_2$ emissions in the design of RC structures similar to those in this study. It is concluded that these relationships vary depending on the ductility class. A similar study [34] shows that the economic cost must be moderately increased to decrease emissions significantly. However, optimizing both objectives is only partially counterproductive, as demonstrated by performing a multi-objective optimization including both criteria [35]. In [8], a comparative study was performed using the economic cost and the environmental impact (involving both EE and $CO_2$ emissions). It was found that any of these objectives leads to good results as measured by the others. However, the best option is to use $CO_2$ emissions since the other indicators keep good levels when using it as the optimization target. For this reason, this study involves the $CO_2$ emissions single-objective optimization of the tri-dimensional frame RC structures shown in Fig. 1. Hence, the objective is to minimize Eq. (7).

$$CO_2 emissions = \sum_{i=1,n} e_i \times m_i(x_1, x_2, \ldots, x_n) \tag{7}$$

Here, $e_i$ represents the unit $CO_2$ emissions (see Table 3), mi are the measurements concerning the construction units in the function of the design variables ($x_1$, $x_2$,…,$x_n$). Table 3 shows unit values of considered materials and activities obtained from the 2016 database of the Institute

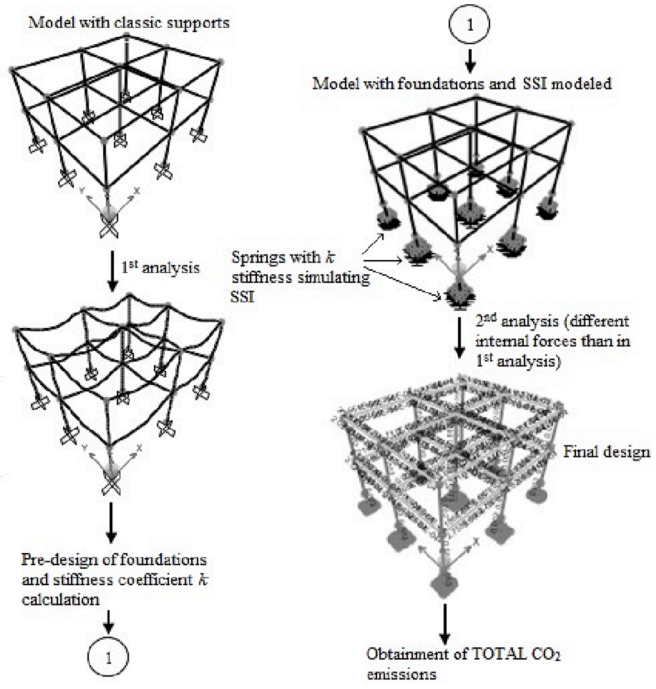


**Fig. 5.** General algorithm for the SSI consideration during structural optimization process.

**Table 3**
Unit $CO_2$ emissions for materials and activities.

| Material | | Units | $CO_2$ em (kg) |
|---|---|---|---|
| Formwork | | $m^2$ | 2.53 |
| Steel (G-60)* | | kg | 3.01 |
| Concrete 25 MPa | | $m^3$ | 244.94 |
| Concrete 30 MPa | | $m^3$ | 279.21 |
| Concrete 35 MPa | | $m^3$ | 305.96 |
| Concrete 40 MPa | | $m^3$ | 307.06 |
| Activities | | | |
| Concrete placement | Beams | $m^3$ | 34.72 |
| | Columns | $m^3$ | 37.20 |
| | Found | $m^3$ | 19.84 |
| Earthwork | Excavation | $m^3$ | 3.99 |
| | Refill | $m^3$ | 12.80 |

* fy=420 MPa, E=220 GPa

of Construction Technology of Catalonia [36]. The $CO_2$ emissions values encompass the use of materials that involve emissions at the different stages of production and placement. Consequently, the higher this value is the lower its sustainability.

As mentioned, all design variables are discrete and can only take relevant values from an engineering point of view. In the case of the frame elements, variables are related to the cross-section dimensions and are limited to multiples of 5 cm. Variables related to foundations rectangularity (L/B, see Fig. 6) can handle nine possible values representing four possibilities for each direction plus the square configuration, e.g., [0.50, 0.63, 0.75, 0.88, 1.00, 1.25, 1.50, 1.75, 2.00]. There are three variables related to this issue. Finally, there are three more variables considering the type of concrete for each group of elements (beams, columns, and foundations), where each one can handle four possible values. The property considered as a variable is the specified compressive strength ($f_c^{'}$). Other properties are also variables (modulus of elasticity, for example), but they depend on $f_c^{'}$, whose values vary in steps of 5 MPa. Table 4 shows the design variables and their corresponding ranges. It is straightforward to note that considering the foundations within the structural assembly (and the corresponding soil-structure interaction) modifies the basic formulation of the problem, where the foundations were not considered [8]. With the addition of 4 more variables, and being the ones related to the foundations' rectangularity very influential in the general formulation, the space of solutions grows exponentially, becoming more challenging to explore and, therefore, to optimize.

On the other hand, this problem involves two fundamental types of constraints. The first group is called *design* (or *explicit*) *constraints*. They are imposed directly on the design variables and function as limits on the movement of these variables. The intervals shown in Table 4 are explicit constraints. They appear for buildability, architecture, functionality, and transportation.

The other group is the so-called behavioral or implicit constraints.

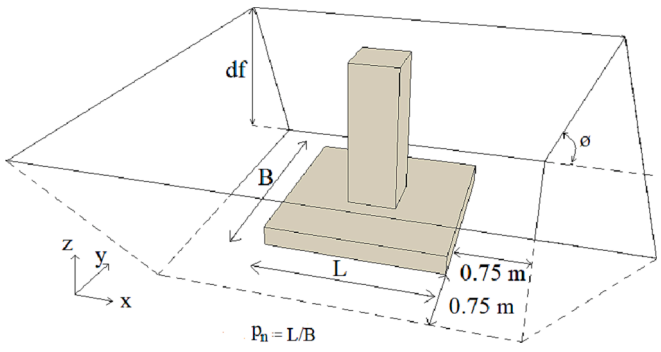


**Fig. 6.** Typical shallow foundation and excavation scheme, p(n) is the rectangularity (variable) [1].

**Table 4**
Design variables and corresponding ranges for each case study.

| Variable | Range | |
|---|---|---|
| | CS-1 and CS-3 | CS-2 |
| Depth of beams of first design group | 300 mm $\leq x_1 \leq$ 600 mm | 400 mm $\leq x_1 \leq$ 700 mm |
| Width of beams of first design group | 200 mm $\leq x_2 \leq$ 300 mm | |
| Depth of beams of second design group | 250 mm $\leq x_3 \leq$ 500 mm | 300 mm $\leq x_3 \leq$ 600 mm |
| Width of beams of second design group | 200 mm $\leq x_4 \leq$ 300 mm | |
| Dimension in x-axis of interior columns | 250 mm $\leq x_5 \leq$ 500 mm | |
| Dimension in y-axis of interior columns | 250 mm $\leq x_6 \leq$ 500 mm | |
| Dimension in x-axis of exterior columns | 250 mm $\leq x_7 \leq$ 500 mm | |
| Dimension in y-axis of exterior columns | 250 mm $\leq x_8 \leq$ 500 mm | |
| Dimension in x-axis of corner columns | 250 mm $\leq x_9 \leq$ 500 mm | |
| Dimension in y-axis of corner columns | 250 mm $\leq x_{10} \leq$ 500 mm | |
| Rectangularity of interior foundations | $0.5 \leq x_{11} \leq 2.0$ | |
| Rectangularity of exterior foundations | $0.5 \leq x_{12} \leq 2.0$ | |
| Rectangularity of corner foundations | $0.5 \leq x_{13} \leq 2.0$ | |
| $f_c^{'}$ in beams | 25 MPa $\leq x_{14} \leq$ 40 MPa | |
| $f_c^{'}$ in columns | 25 MPa $\leq x_{15} \leq$ 40 MPa | |
| $f_c^{'}$ in foundations | 25 MPa $\leq x_{16} \leq$ 40 MPa | |

They are sometimes referred to as state equations. These constraints fulfill the design limit states, i.e., defining the values the variable parameters must meet to satisfy behavioral requirements. In structural optimization, the behavioral constraints are usually set by design standards. Eq. (8) represents the classical formulation of behavioral constraints.

$$g_j(x_1, x_2, \ldots, x_n) \leqslant 0 \tag{8}$$

Constraints related to the strength (ultimate) limit state for RC frame elements are automatically satisfied through the API SAP2000-MATLAB platform (calculus of the reinforcing steel area), which computes the structural design according to the standards. The geotechnical and structural design of the foundations is implemented in a routine programmed in MATLAB according to the Eurocode. It is essential to note that this problem is formulated with a deterministic approach, so the design is based on the Limit States method. Therefore, aspects such as the variability of soil parameters are considered when applying the different safety coefficients. On the other hand, constraints related to serviceability limit state accomplishment are deflections in beams, limit displacement at the top of the building, or cracking of concrete members. As mentioned, these constraints are produced by applying the standards. The way to verify these behavioral constraints is that when any of them is not fulfilled, the value of the objective function for the current solution is penalized so that the algorithm discards it as possible. For more detailed information on how the deterministic approach works and the implementation of the constraints, refer to the document [1].

### 2.4. Solution of the optimization problem

Two main strategies are used to solve the formulated problem. The first presents a classical heuristic approach using a relatively new Biogeography-based Optimization (BBO) strategy. The second relies on kriging formulation metamodels to optimize surrogate models and avoid costly accurate simulations, using the BBO strategy as the basic optimization algorithm. It should be noted that the optimization of this type

of problem is a complex process in which it is not guaranteed to find the global optimum. In addition, meta-heuristic optimization based on metamodels is proposed as an alternative to conventional optimization. It is intended to significantly reduce computational costs while maintaining the quality of the solutions.

### 2.4.1. Conventional heuristic optimization

Heuristics are the most implemented strategies to solve structural design optimization problems. It is precisely the case for optimization problems in the design of RC structures. In the optimization of simple elements (beams or columns), several heuristics have been used, such as Harmony Search (HS) [37,38] or Glowworm Swarm Algorithm [39]. Genetic Algorithms (GA) have been implemented for the solution of the optimization of RC plane frames [40,41], as well as HS [42] or Simulated Annealing (SA) [9,43]. On the other hand, to solve optimization problems of three-dimensional concrete structures, it has been implemented Particle Swarm Optimization (PSO) [14,15], the Flower Pollination Algorithm [17], the Cascade Optimization Method [18], HS [44], SA [45,46], or the old bachelor algorithm [47].

Alternatively, there is a heuristic of relatively little diffusion called Biogeography-based Optimization, proposed by [48] and, although ephemeral, has been used in problems of optimal design of civil engineering structures. In [49], it is implemented a version of BBO with Levy flight distribution (LFBBO) in the design optimization of cantilever retaining walls. In [50], BBO is used to optimize the design of 3D and plane frame steel structures. In the case of RC structures, BBO has been successfully implemented to solve a design optimization problem. In [21,51], BBO was compared to other heuristics in these types of problems, outperforming some classical ones such as GA, HS, or PSO. In [1], the main parameters of BBO were tuned to deal with problems related to the formulated in this paper. Finally, in [8], BBO was implemented to optimize the design of the same structure of this paper without considering foundations and SSI during modeling.

As mentioned, previous works have demonstrated the superiority of BBO over other methodologies to solve this type of problem. However, considering the benefits of working with metamodels, an experiment is carried out to select the best heuristic that will be the basis of the meta-heuristic algorithm. In addition, it will serve as a reference to compare and validate the results of the proposed meta-heuristic. The other two heuristics tested are GA and PSO. Note that the parameters of the methods are selected according to the recommendations provided in [51]. Fig. 7 shows the behavior of each method in the optimization of the real model (the *equis* represent the values obtained in three tests) and of a metamodel (the boxplots represent the statistical analysis of twenty tests) created using the basic Kriging methodology (see next section). A polynomial of order 0 is used as the regression model to construct the metamodel. The utility (or measure used to compare the performance of each method) is the final value obtained in each optimization process. The figure shows that BBO is superior in both types of optimization, especially in the real model. It also shows that using metamodels is an excellent alternative to perform parameter tuning processes and compare options to give a solution to a real problem using a surrogate model. In this case, this metamodel (created using a polynomial of order 0, see next section) could be more precise regarding values. Even so, it captures the fundamental characteristics of the natural phenomenon and is much more computationally low-cost to evaluate. It is highly desirable in parameter setting or comparison of alternatives to solve real problems.

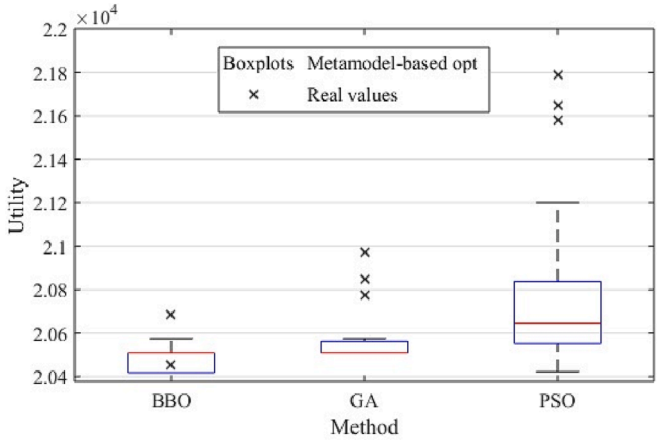


**Fig. 7.** Comparison of the performance of the three heuristics in optimizing the real model (*equis*) and the surrogate model (boxplots, where bottom whisker, box bottom, middle, top, and top whisker denote the minimum, 25th percentile, median, 75th percentile and maximum utility of each process).

The BBO algorithm represents mathematical models of how species migrate from one island to another, how new species arise, and how species become extinct. A more detailed explanation of the BBO strategy can be found in [1,8,48]. In order to explain why BBO seems to be a proper strategy for dealing with discrete optimization problems, it is essential to highpoint the main difference between this strategy with classical Evolutionary Algorithms (EAs), such as GA, for example. It is associated with the recombination operator. When classical EAs combine complete solutions, the BBO algorithm processes solutions from variable to variable (not solution to solution). That is to say, when GA combines two solutions to create a new one, BBO can obtain solutions from more than two previous solutions. In addition, the combination and the mutation operators can affect the variable involved in the same process of getting new solutions.

Highlight that one of the advantages of BBO over other heuristics is the rapid convergence to outstanding solutions very quickly. It is especially desirable in these extremely computationally expensive processes. One of the reasons for this fast and efficient convergence is the algorithm's effectiveness with relatively low population sizes. For example, in the parameter tuning process mentioned above, the optimal population size was 80 individuals, while for the other two heuristics, it was around 200. More information on this aspect can be found in [1].

### 2.4.2. Kriging-based optimization

Conventional heuristic optimization processes are usually quite computationally expensive, even when using a tuned method with fast and efficient convergence, such as BBO. Alternatively, MASDO allows for reducing computational consumption. The basic idea consists of using a surrogate model (instead of the real and complex one) built from an initial sampling of points. This surrogate model can predict the output data (objective response) from any input data (design variables) in the design space.

There are three main steps to building a metamodel: (1) selection of the initial sample of points inside the design space, also called *the design of experiment* (*DoE*), (2) construction of the approximate mathematical model using the initial sample of points using a metamodeling technique and (3) validation of the constructed surrogate model. The main objective of the metamodel construction is to obtain a model that predicts the actual response with the best possible accuracy [5].

To select the initial sample of points to construct the metamodel (DoE), the sample size and the position of these points must be considered. On the one hand, the sample size (N) is directly related to the number of variables. On the other hand, once the number of points has been selected, they should be placed in such a way as to gather as much information as possible. DoE can be split into two main groups. Classic designs tend to place the sample points around the border of the design space and only locate a few points inside it [52]. The other group, called space-filling designs, is more suitable for building advanced metamodels. One of the popular ones is Latin Hypercube Sampling (LHS).

In this work, the DoE will be performed through LHS. The effectiveness of this technique has been proved in several studies [53]. LHS was proposed by [54]. This method determines the N number of non-

overlapping intervals for each variable from several design variables (v) and some initial input sample points (N). Then, the design space is distributed in Nv sections. Each point is placed in such a way as to correspond to a combination of different intervals of each variable design range. Consequently, LHS designs ensure all design variables are represented with their intervals [5].

Once the appropriate set of points has been selected and the corresponding high-fidelity simulations for each point have been performed, the next step is to choose a metamodel and fitting strategy. As mentioned, NN and Kriging strategies are the most implemented techniques in structural engineering. However, NN-based models usually require several sample points and considerable computational time to train the network [55]. On the contrary, Kriging-based models are flexible strategies and less time-consuming than NN-based techniques [56]. For this reason, the metamodel construction in this study is based on the Kriging formulation and the DACE Kriging Toolbox V 2.0 [57]. Kriging models are extensive and very popular global approximation techniques based on the work of Daniel G. Krige [58], adapted to handle geostatistical problems [59]. A more detailed explanation of the Kriging formulation can be found in [57,60].

### 2.4.3. Simple Kriging-based optimization

The usual methodology of Kriging-based optimization starts with generating the N initial sample points using the LHS technique. It is necessary to obtain the real fitness value of each point. Then, the metamodel is built according to the mathematical strategies used by Kriging-based approaches. It is also important to highlight that each metamodel type has its associated fitting model. In this case, the hyperparameters used to fit the model are determined by maximum likelihood estimation [60]. Once the metamodel has been built, it is necessary to validate it. For this purpose, measurements based on error estimation are usually used. In this case, the mean absolute percentage error (MAPE) is implemented, measured using ten randomly obtained points (that do not coincide with those obtained in the DoE) as shown in Eq. (9).

$$MAPE = \frac{\sum_{i=1}^{n} \frac{|y_i - \hat{y_i}|}{y_i}}{n} \times 100\% \tag{9}$$

Here, $n$ is the number of points used for the measurement (ten in this case), while $y_i$ and $\hat{y}_i$ are the actual and predicted values, respectively. This MAPE value must be lower than a previously established threshold. If this criterion is not met, another ten randomly selected points (that do not coincide with any previous point) are added. The process is repeated until this condition is met, i.e., the metamodel has adequate accuracy. Then, the optimization process proceeds. For this case, the BBO algorithm explained above is used. This algorithm optimizes the response surface generated by the metamodel. Once the "optimal solution" of the metamodel has been found, it is necessary to check if it is feasible using a high-fidelity simulation. If the solution is not feasible, it is penalized with a coefficient of penalization CP. This point is added to those used to build the initial metamodel. If the solution is feasible, it is taken as the optimal solution.

One value that defines and regulates the process's accuracy is the coefficient of penalization CP applied to infeasible solutions, which is common in this type of optimization problem. Even more significantly, the best solutions are often close to these "not feasible" points. Therefore, a sensitivity analysis is conducted to observe the strategy's behavior for different CP values. Fig. 8(a) shows the results of studying three values: 1.00 (no penalization), 1.15, and 1.30. In this case, an initial number of sampling points of N = 100 is considered. Five tests are performed for each penalty coefficient, and the mean of the five values is plotted. The figure shows that as the penalization coefficient increases, the accuracy of the metamodel decreases. Therefore, CP = 1 is used for the simple Kriging-based optimization.

On the other hand, another essential aspect is the number of initial points N obtained in the DoE. A sensitivity study similar to the previous one is carried out. Five values are analyzed: 20, 50, 100, 200, and 300. Five tests are performed for each value, and the average of these values is plotted. Fig. 8(b) shows that the MAPE values are outstanding. It indicates that the metamodels obtained from the points located by LHS are pretty accurate.

However, simple Kriging-based optimization often produces unsatisfactory results, as optimal values tend to be located at the extremes of the variables, especially the lower ones. It frequently leads to constraints being violated, requiring additional points to be added to the initial sampling from which the first metamodel was created. Without a coefficient of penalization (CP), the algorithm may repeatedly select the same point as the optimal solution, even if it fails to meet the constraint requirements. However, the solution found in such cases could be better, consisting mainly of variables with extreme values. Increasing the CP results in a "see-saw effect", affecting the area surrounding the infeasible point and all other values. Therefore, when optimizing the metamodel, if the obtained point violates constraints, the optimum becomes the opposite value through penalization (see-saw effect). It is usually the case for variables most affected by constraint violations, such as beam depths or column section dimensions.

Thus, the points obtained by LHS produce a highly accurate metamodel only within the interior of the solution space, as illustrated in Fig. 9. This situation becomes more intricate for the problem since there are too many variables compared to the limited number of possible values they can handle. In other words, the interior solution space is minimal compared to the points at the boundaries, which causes the "see-saw effect". Moreover, since meaningful solutions are often found at these frontier points, this explains the outcome when applying simple Kriging-based optimization to the problem.

### 2.4.4. Kriging-based meta-heuristic optimization

Considering the limitations of the simple strategy to deal with the

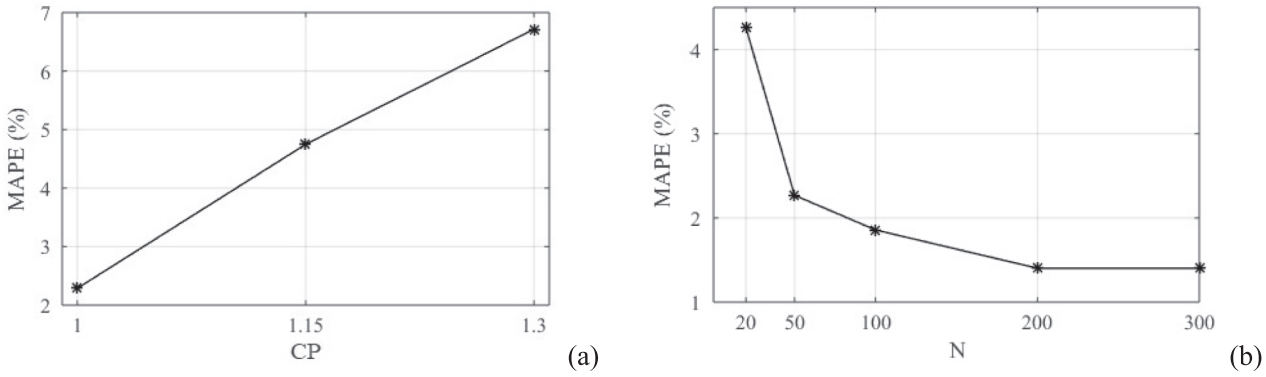


**Fig. 8.** Study of (a) the coefficient of penalization (CP) and (b) the initial sampling size ($N$).

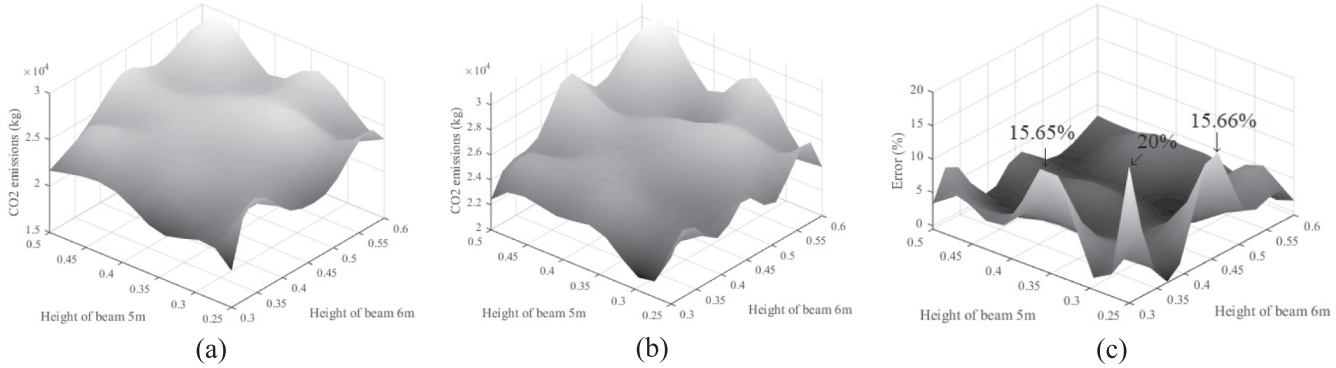


**Fig. 9.** Example of the low effectiveness of the metamodel at the boundaries of the solution space, (a) simulated response, (b) real response and (c) error between the simulated and the real. Coefficient of penalization equal to 1.00. The values of the other variables are randomly selected.

formulated optimization problem, a two-phase strategy based on Kriging metamodels is designed. It also includes concepts of online optimization and a local search heuristic. The global strategy is called Kriging-based meta-heuristic optimization (KBMO).

Using only LHS is not a good choice for this type of problem, although it provides excellent results in the interior of the solution space. Therefore, a DoE is designed using points obtained through LHS and others arbitrarily located at the boundaries. The basic idea of this strategy is the following: to perform a first exploration of the solution space to "detect" promising areas using a general metamodel; to build a "local" metamodel in the most feasible area; to optimize the "local" metamodel and to obtain the best solution resulting from the use of metamodels (two-phase Kriging-based strategy). From this point, a local search heuristic using the actual response surface is applied to improve the solution obtained using the surrogate models. The steps are as follows (see Fig. 10):

1. The initial DoE is designed by obtaining 20 points using LHS, 32 exterior points, and 16 corner ones for 68 initial points. Two exterior points are obtained for each variable (one upper and one lower), thus the 32 exterior points. An exterior point is considered to be one in which the value of a variable is fixed at one of the extremes while the other variables take random values. A corner point is considered to be set to an extreme value. At the same time, the other variables take

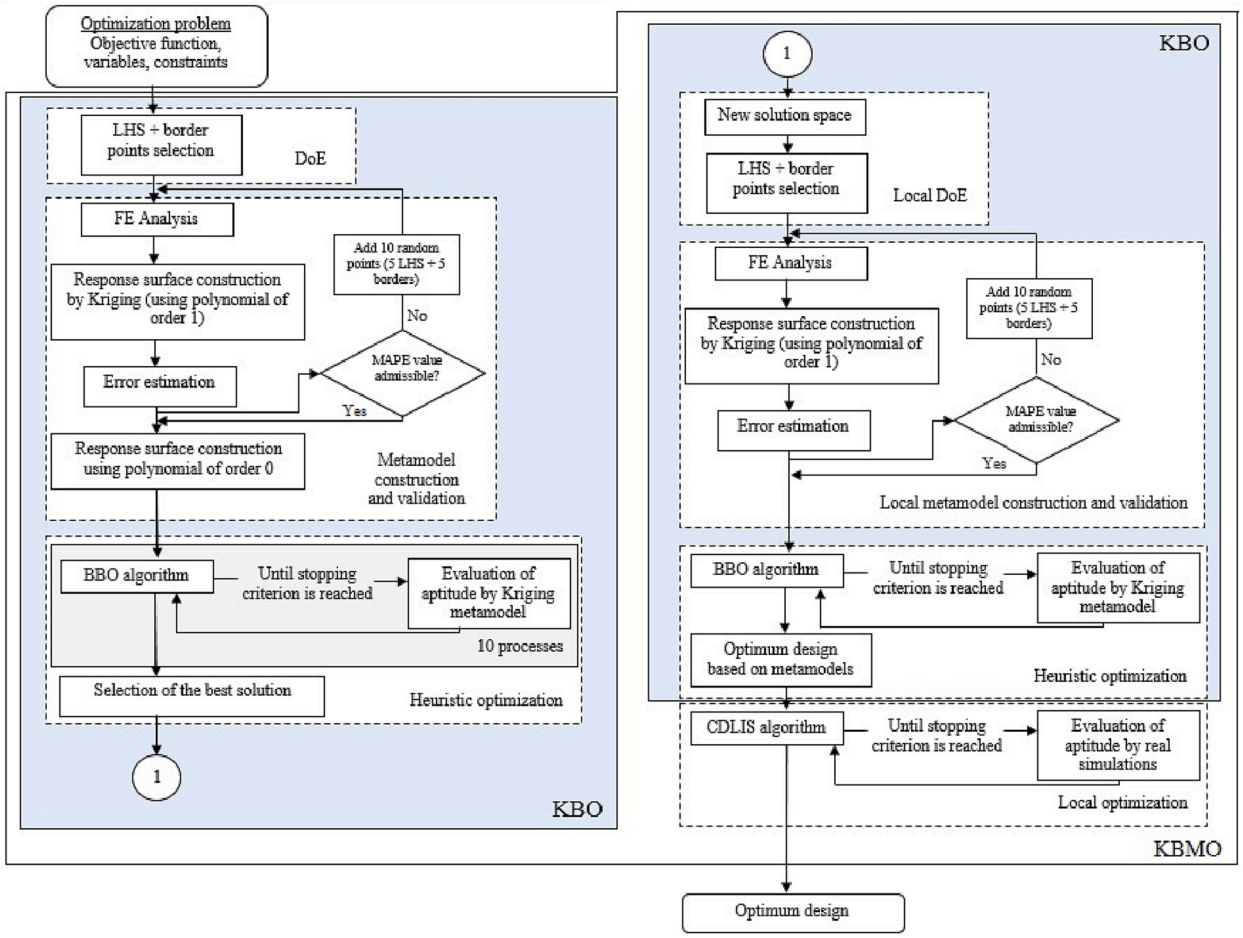


**Fig. 10.** Flowchart of Kriging-based meta-heuristic optimization (KBMO).

a random value from the two extremes that correspond to each one, i.e., all variables have extreme values. Since fewer corner points exist, only 16 are considered, one for each variable. Then, the high-fidelity simulation is performed for each point. The metamodel is created using a first-order polynomial for the regression model (see how Kriging works in suggested references). The metamodel is "validated" using ten randomly selected points (five interior ones obtained through LHS and five exterior-corner ones) and the corresponding MAPE. If the MAPE value is not less than 6%, these 10 points are incorporated into the initial DoE, and the metamodel is updated. The process is repeated until the criterion is met. Once a good sample of initial points is obtained, another metamodel is created with this sample, using a polynomial of order 0 (constant). It creates a less accurate metamodel than the one obtained with the first-order polynomial, but the "see-saw effect" does not affect it.

2. The metamodel is optimized with the simple BBO heuristic. The generated response surface is quite complex, i.e., each optimization process usually gives different results, although with much better quality than those obtained with the metamodels built using a first-order polynomial. Ten optimization procedures are performed, which, when using the metamodel, present a little computation time compared to the accurate simulations. The best solution is selected from the ten obtained.
3. A new local solution space is created by adding one value up (+1) and one value down (-1) to the "optimal" values of each variable using this solution. If the value of a variable is located at the extreme, two units are added or subtracted so that each variable can take three values. Using similar criteria as in point 1, a new DoE is created (10 LHS points, 15 exterior, and 10 corner points, for a total of 35 points), and the "local metamodel" is created this time using a first-order polynomial as the regression model. The accuracy of the metamodel is checked with ten selected points following the same criteria as point 1 until it meets the established criteria.
4. This metamodel is optimized using the simple BBO strategy. Until here, this part of the process is named Kriging-based optimization (KBO).
5. Considering that the computation time is still relatively low compared to the conventional procedure, the process is finished with the local optimization algorithm (CDLIS, see Fig. 11), starting from the point obtained using the metamodels. The final solution is considered the optimal one.

It is essential to highlight that each of the high-fidelity simulations performed in the process is stored so that if a point is repeated, it is unnecessary to perform costly extra simulations.

On the other hand, the local search algorithm is based on strategies such as the Simplex Nelder-Mead algorithm [61] and Integer Linear Programming [62]. It consists of performing discrete unit steps and gradually storing the results to improve the analyzed solution. The steps are as follows (see Fig. 11):

1. Each variable increases and decreases by one unit in value, starting from the basic solution. Then, the corresponding high-fidelity simulation is run, and the results are stored. If the variable's value is in one of the limits, it is not violated, so only one solution is analyzed. In addition, each new solution is checked in the database against all previous solutions to avoid repeating additional costly accurate simulations. If already performed, it is not necessary to run the FE software. Therefore, each iteration will have at most twice the number of variables.
2. Once all the results are stored, the new solution is formed, updating the values of each variable that improved the basic solution. For example, in Fig. 11, variable 1 improved the solution by decreasing

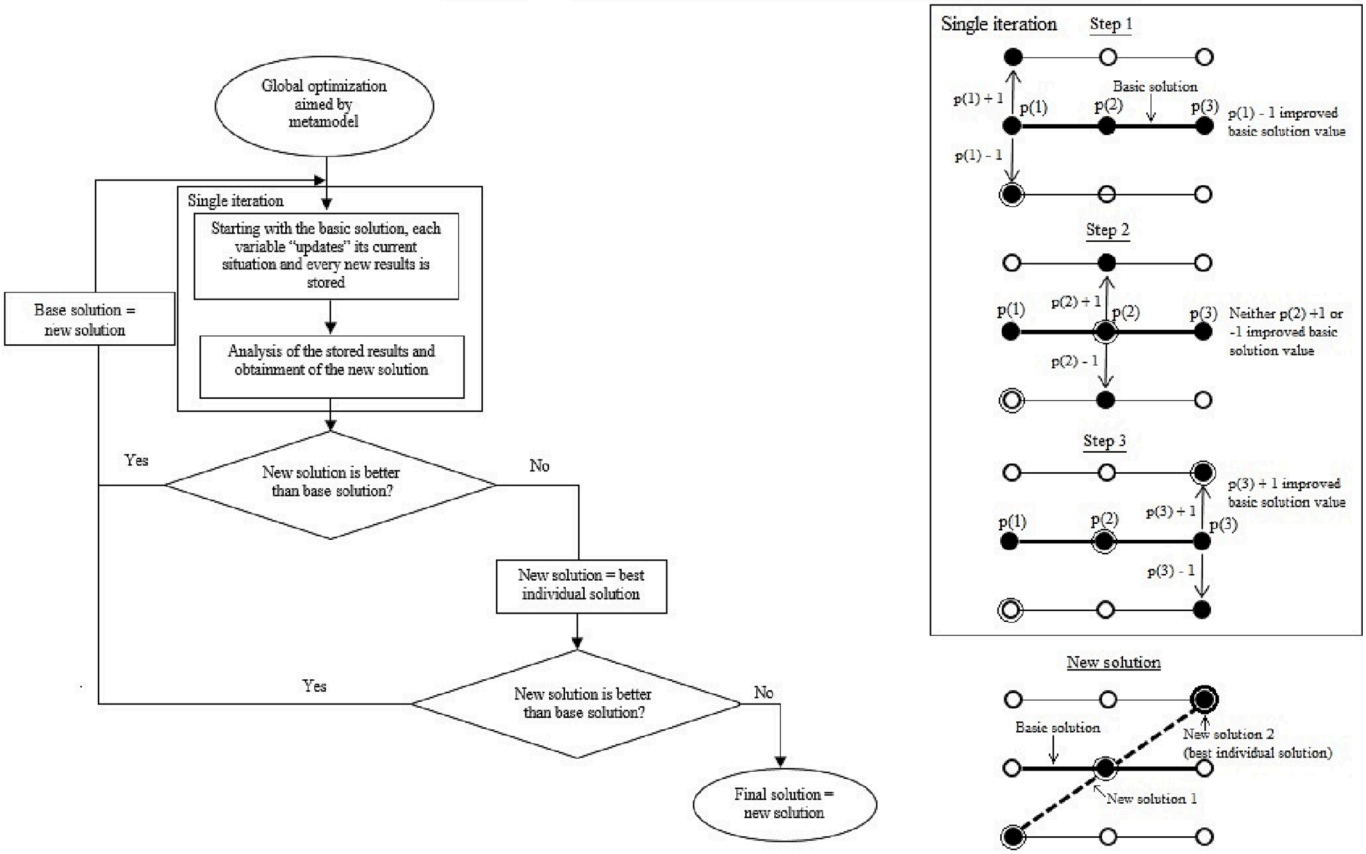


**Fig. 11.** Flowchart of Constrained Deterministic Local Iterative Search (CDLIS). Left: general flowchart. Right: example of an iteration in a problem with 3 variables.

its basic value (p(1)-1), and variable 2 did not improve with either step. Variable 3 improved by increasing it (p(3)+1), so the basic solution [p(1), p(2), p(3)] becomes [p(1)-1, p(2), p(3)+1]. It is called new solution 1. In addition, the best individual solution is identified, which is the best solution of all those obtained during the iteration. It is the new solution 2.

3. The high-fidelity simulation obtains the actual value of the objective function provided by new solution 1. If this value improves the value of the basic solution, the new solution 1 becomes the basic, and a new iteration begins.
4. If the value of solution 1 does not improve the base one, the quality of the new solution 2 (already stored) is analyzed. If this new solution is better than the basic one, the latter becomes the new solution 2 (single best solution), and a new iteration begins. If the new solution 2 does not provide a better result, the process is ended, and the basic solution is considered the optimal global solution.

## 3. Results and discussion

The results and their discussion focus on two fundamental aspects: the influence of considering the SSI and the application of the proposed metamodeling strategy. The methodology is based on performing the basic experiments on case study 1 and validating the results with the other two models. Additionally, this type of structure's behavior is analyzed by the different conditions generated in this study.

### 3.1. Influence of SSI consideration

The results' first point focuses on including the SSI during modeling. For this purpose, the three case studies are optimized by considering classical (fixed) supports and the SSI using the two soil types. In addition, the optimization with classical supports does not consider the environmental cost of the foundations in the objective function, unlike the optimization considering the SSI. As mentioned, the primary hypothesis is that a structure modeled with SSI will have a more stressed superstructure due to the logical differential settlements between contiguous supports.

Table 5 shows the optimum values of the variables for each model. It can be appreciated that the results are different for each support condition, although some aspects maintain their tendency. For example, corner columns tend to be square or with little rectangularity in the direction of predominant bending due to gravitational loads ("x" axis in these cases). This rectangularity tends to increase in soil 2, where differential settlements are higher. As do corner columns, exterior columns usually have rectangular cross-sections with the most significant dimension on the x-axis. Here the rectangularity is generally more significant. The interior columns usually have a rectangular section with a larger side in the y-axis direction. It is to increase the horizontal stiffness of the structure in that direction, which is critical against wind action. Note that these columns do not have predominant bending due to gravitational loads since the structures are symmetrical.

On the other hand, the interior foundation, which does not receive a predominant bending moment due to gravitational loads, tends to be designed with a rectangular footing to deal with the horizontal wind load in its critical direction. Exterior foundations usually have square footings. Corner foundations tend to be designed with a rectangular base with a larger dimension on the x-axis to cope with gravity loads. It can be seen how there is a match between the columns and the corresponding foundations. Regarding the quality of the concrete, the elements that work primarily in bending (beams and foundation footing) require concrete with low compressive strength. On the other hand, since this property ($f_c^{'}$) is significant in columns, the best choice is usually high-strength concrete.

**Table 6**
Comparison of results of optimization procedures with and without considering soil-structure interaction during modeling (using CS-1*).

| | Elements | | No SSI | | SSI (soil 1) | SSI (soil 2) |
|---|---|---|---|---|---|---|
| $CO_2$ emissions (kg) | Beams | Steel | 2917 | | 3223 | 3274 |
| | | Concrete | 3155 | | 2584 | 2584 |
| | | Formwork | 352 | | 301 | 301 |
| | | Total | 6424 | | 6108 | 6159 |
| | Columns | Steel | 1968 | | 2838 | 3024 |
| | | Concrete | 1333 | | 1952 | 2345 |
| | | Formwork | 175 | | 193 | 234 |
| | | Total | 3476 | | 4983 | 5603 |
| | Superstructure | | 9900 | | 11 091 | 11 762 |
| | Foundations | | Soil 1** | Soil 2** | | |
| | | Steel | 2694 | 1539 | 2613 | 1062 |
| | | Concrete | 872 | 427 | 868 | 476 |
| | | Formwork | 77 | 68 | 81 | 80 |
| | | Earthwork | 5867 | 5014 | 5801 | 4963 |
| | | Total | 9510 | 7048 | 9363 | 6581 |
| | TOTAL | | 19 410 | 16 948 | 20 454 | 18 343 |

* Results of CS-2 and 3 are graphically represented in Fig. 12.
** Foundations are designed and their environmental cost is calculated for the optimal solution (model with classic supports, no SSI).

**Table 5**
Design variables and corresponding optimal values for each case study.

| Variable | Optimal values | | | | | | | | |
|---|---|---|---|---|---|---|---|---|---|
| | CS-1 | | | CS-2 | | | CS-3 | | |
| | No SSI | Soil 1 | Soil 2 | No SSI | Soil 1 | Soil 2 | No SSI | Soil 1 | Soil 2 |
| $x_1$ (m) | 0.45 | 0.35 | 0.35 | 0.60 | 0.45 | 0.50 | 0.45 | 0.45 | 0.50 |
| $x_2$ (m) | 0.20 | 0.20 | 0.20 | 0.25 | 0.25 | 0.25 | 0.20 | 0.25 | 0.25 |
| $x_3$ (m) | 0.40 | 0.35 | 0.35 | 0.40 | 0.35 | 0.35 | 0.40 | 0.35 | 0.35 |
| $x_4$ (m) | 0.20 | 0.20 | 0.20 | 0.25 | 0.25 | 0.25 | 0.20 | 0.25 | 0.25 |
| $x_5$ (m) | 0.30 | 0.30 | 0.25 | 0.25 | 0.30 | 0.30 | 0.30 | 0.30 | 0.30 |
| $x_6$ (m) | 0.25 | 0.40 | 0.35 | 0.45 | 0.40 | 0.45 | 0.45 | 0.40 | 0.45 |
| $x_7$ (m) | 0.35 | 0.35 | 0.45 | 0.35 | 0.50 | 0.50 | 0.40 | 0.50 | 0.50 |
| $x_8$ (m) | 0.25 | 0.25 | 0.30 | 0.25 | 0.25 | 0.30 | 0.25 | 0.25 | 0.30 |
| $x_9$ (m) | 0.25 | 0.30 | 0.35 | 0.25 | 0.40 | 0.50 | 0.25 | 0.40 | 0.50 |
| $x_{10}$ (m) | 0.25 | 0.30 | 0.40 | 0.25 | 0.35 | 0.35 | 0.25 | 0.35 | 0.35 |
| $x_{11}$ | – | 0.75 | 0.63 | – | 1.00 | 1.25 | – | 1.00 | 0.88 |
| $x_{12}$ | – | 1.25 | 1.00 | – | 1.00 | 1.00 | – | 1.00 | 1.00 |
| $x_{13}$ | – | 1.00 | 0.75 | – | 1.25 | 1.50 | – | 1.25 | 1.25 |
| $x_{14}$ (MPa) | 25 | 25 | 25 | 25 | 25 | 25 | 25 | 25 | 25 |
| $x_{15}$ (MPa) | 25 | 40 | 25 | 40 | 40 | 40 | 40 | 40 | 40 |
| $x_{16}$ (MPa) | – | 25 | 25 | – | 25 | 25 | – | 25 | 25 |

Table 6 highlights the differences in the designs with and without SSI. It is constructed with the basic case study (CS-1) results. First, it is observed that the superstructure of the models optimized with SSI is much more environmentally costly than that of the model with classical supports: 12.03% for soil 1 and 18.81% for soil 2. It does not mean that not including the SSI is better. On the contrary, using a model with classical supports does not consider additional stresses introduced into the structure, which is why its optimal design is "less costly". When modeling the system with SSI, the optimal results are more expensive because the superstructure is more stressed. Thus, the elements are designed with more material. Therefore, the design of a model that does not consider the SSI does not cause the collapse of the structure but rather a gradual and accelerated deterioration because of the appearance of stresses for which it was not designed. It causes a considerable increase in the use of resources for its maintenance. It should be remembered that support settlements are a slow process that could take years to reach its final stage. On the other hand, obtaining a more costly superstructure for soil 2 proves the hypothesis in section 2.2.1 about the increase in internal forces resulting from differential settlement, which is higher for these types of soils.

On the other hand, it can be seen that the costs of the beams do not vary much from one model to another, the columns being the main ones affected. Differential settlements cause an increase in the bending moment. This increase directly affects the beams. It is also transferred to the columns due to how statically indeterminate structures work (as in this case). Therefore, the beams' design does not "suffer" too much from this increase in bending since they are elements intended to support this stress. However, columns are intended to support axial stress fundamentally, so this increase in bending resulting from the consideration of the SSI does significantly affect their design. It causes a significant increase in the dimensions and rectangularity of the columns' cross-sections and the need for reinforcement to deal with these internal forces more efficiently. Table 6 shows that for soil 1, the cost of the columns in comparison with the model using classic supports increases by 43.35% (46.55% for concrete and 44.21% for steel), while for soil 2, the increase is 61.19% (75.92% for concrete and 53.66% for steel).

Fig. 12 shows the graphical representation of Table 6. In addition, the results of case studies 2 and 3 are included. Here we can see how the conclusions obtained using the CS-1 are reaffirmed. As can be seen, there is a tendency to increase the absolute differences in the superstructure design. In the case of CS-2, although the absolute differences increase compared to CS-1, their ratio expressed as a percentage of the model without SSI decreases due to higher total emissions. However, it can be seen how in CS-3, this ratio shoots up. Here it can be concluded that as the number of levels increases, the consideration of SSI becomes even more significant. It is due to the increase in axial forces and differential settlements. Furthermore, the predominantly frictional soil is the most influential, obeying the theories discussed in Section 2.2. The figure also confirms the significant influence of the columns on the differences observed for each support condition. It is magnified in CS-3 due to increased differential settlements and bending in the superstructure. Thus, it is confirmed that this increase in bending resulting from the SSI phenomenon significantly influences the design of the columns.

### 3.2. Application of KBMO

Conventional optimization using FE software as a computational engine for modeling, analysis, and structural design is highly costly. For these reasons, the results will be measured in terms of the accuracy of the metamodel-based strategy compared to conventional optimization, highlighting the savings achieved in computational time. The element considered in the analysis of KBMO is the coefficient of penalization CP. It is important to remember that optimization based on metamodels aims to reduce computational costs while maintaining good results. In this section, we use the models with SSI (with both soils) to test the effectiveness of the proposed methodology.

#### 3.2.1. Obtaining the appropriate CP

As mentioned above, an aspect of significant importance in implementing metamodel-based optimization is the coefficient of penalization applied to infeasible solutions. Therefore, the study of applying the KBMO methodology starts with searching for the appropriate CP. Case study 1 is used for this purpose.

*3.2.1.1. Predominantly cohesive soil.* Table 7 and Fig. 13 show how, in general, the results are better for low CPs. It is because, as proved in section 2.4.2, more accurate predictions are obtained for low CP values. It occurs in both strategy steps: the Kriging-based optimization (KBO) and the completion with the local heuristic technique. The final results are the best in the case of CP=1.15, even if the KBO offers the worst. The response surface generated with this value of CP presents a zone of good local optima corresponding to an area of the real surface close to the global optimum. On the other hand, it can be said that the most stable values were obtained for a CP=1.05 since both results (intermediate and final) are excellent. This configuration also offers the most significant computational savings.

In Fig. 13, the final results are pretty accurate. Three CP configurations have above 98% accuracy compared to CO. The cases of CP equal

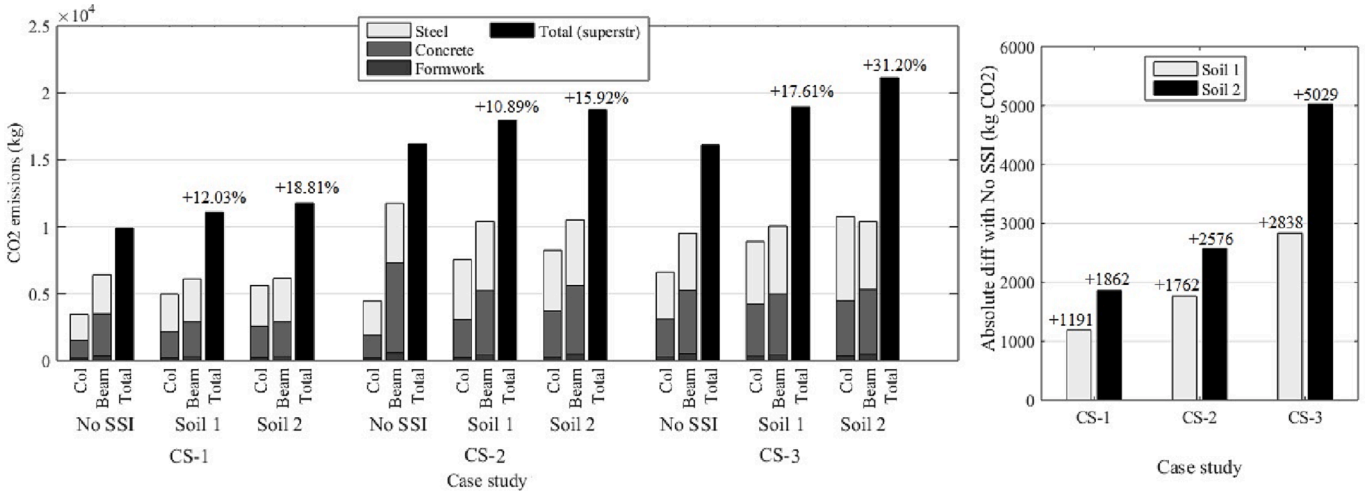


**Fig. 12.** Graphical representation of the results referring to SSI consideration's influence on the superstructure. Left: Results shown in Table 6 and those obtained with CS-2 and 3. Right: Absolute differences for each case study and each soil type compared to the model without SSI.

**Table 7**
Overview on results of applying the proposed metamodeling strategy in comparison with Conventional Optimization (CO) of the model considering SSI for the predominantly cohesive soil.

| Method | CP | Mean results | | | | Best results | |
|---|---|---|---|---|---|---|---|
| | | Time (s) | Comp. time savings (%) | $CO_2$ emissions (kg) | Accuracy with respect to CO (%) | $CO_2$ emissions (kg) | Accuracy with respect to CO (%) |
| KBMO | 1.03 | 10 840 | 91.97 | 20 786 | 98.76 | 20 511 | 99.72 |
| | 1.05 | 10 706 | 92.07 | 20 902 | 98.20 | 20 717 | 98.71 |
| | 1.10 | 15 930 | 88.20 | 21 243 | 96.53 | 20 727 | 98.67 |
| | 1.15 | 15 255 | 88.70 | 20 684 | 99.26 | 20 454 | 100.00 |
| | 1.20 | 14 351 | 89.37 | 21 495 | 95.31 | 21 346 | 95.64 |
| Conv. Opt. (CO) | | 135 000 | | 20 532 | | 20 454 | |

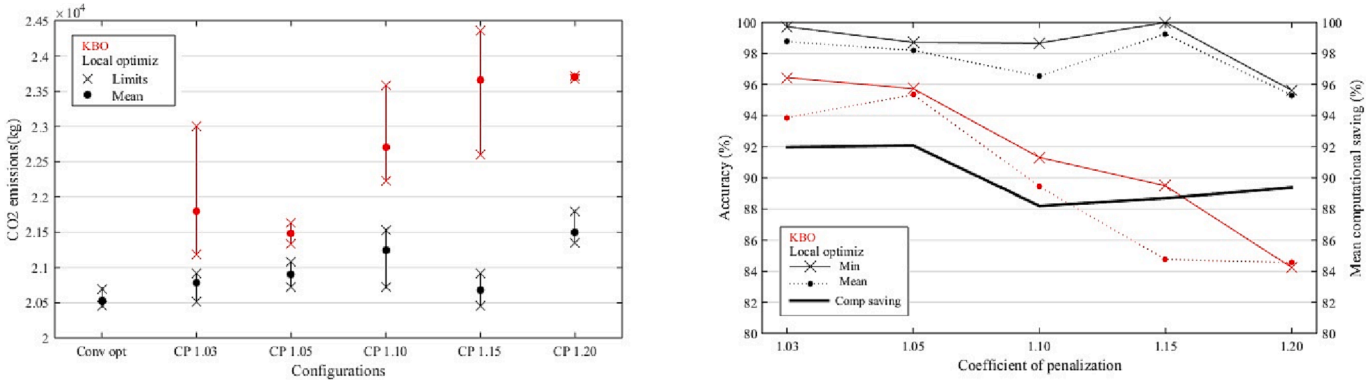


**Fig. 13.** Graphic comparison of results shown in Table 7. Left: simple box plots (extreme values and mean) of three test performed for each configuration. Right: Accuracy of metamodel-based optimization results (in comparison to CO) for different CPs (left y-axis) and corresponding computational savings (right y-axis).

to 1.03 and 1.05 are pretty outstanding, considering not only the final results but also those obtained with the KBO. Note that one of the three tests with CP=1.03 obtained a result accuracy of 99.72% compared to the best solution obtained by the CO, being this value even better than one of the three results obtained by the conventional method. The best value found with CP=1.05 has an accuracy of 98.71%, another excellent result. On the other hand, this figure shows the computational savings obtained. This saving lies almost entirely in substituting high-fidelity simulations with metamodels. The number of high-fidelity simulations is determined by the number of simulations needed to obtain a first surface with a MAPE lower than 6% (step 1) and by the number of iterations the local search algorithm must do to find the best solution. The latter is influenced by the quality of the solution obtained at the end of the KBO. Low CPs offer much more computational savings because of their more accurate surrogate response surfaces and better intermediate solutions. In general, using low CPs (1.03 and 1.05) saves, on average, almost 92% of computational time, with very accurate results compared to CO.

*3.2.1.2. Predominantly frictional soil.* Table 8 and Fig. 14 show that the intermediate (KBO) and final results (KBMO) are less efficient. It is because this model using soil 1 is more "unstable", where there are certainly more constraint violations in a more deformed and stressed superstructure. It makes the actual response surface more difficult to predict. The results with the lowest CP (1.03) are remarkable, which are poor compared to those obtained for soil 1. It is due to the previous approach to the number of constraint violations, where this low penalty seems less efficient in predicting the real phenomenon. Again, the results with CP= 1.15 lead to reasonably good final results since both models, even with different soils, should have similar overall behavior. It should be noted that the best solution was obtained with CP=1.05, with an accuracy of 99.24%. The computational savings were also lower due to obtaining less accurate metamodels. Overall, the results are still quite satisfactory.

### *3.2.2. Application of KBMO with CP=1.05 to case studies 2 and 3*

Having concluded that the best option for penalizing infeasible solutions is to apply a CP of 1.05, it is tested the proposed strategy with case studies 2 and 3. Fig. 15 shows the results for the three cases. Part (a)

**Table 8**
Overview on results of applying the proposed metamodeling strategy in comparison Conventional Optimization (CO) of the model considering SSI for the predominantly frictional soil.

| Method | CP | Mean results | | | | Best results | |
|---|---|---|---|---|---|---|---|
| | | Time (s) | Comp. time savings (%) | $CO_2$ emissions (kg) | Accuracy with respect to CO (%) | $CO_2$ emissions (kg) | Accuracy with respect to CO (%) |
| KBMO | 1.03 | 12 877 | 90.17 | 19 002 | 96.59 | 18 715 | 97.97 |
| | 1.05 | 14 764 | 88.73 | 18 646 | 98.53 | 18 483 | 99.24 |
| | 1.10 | 15 629 | 88.07 | 18 981 | 96.71 | 18 885 | 97.05 |
| | 1.15 | 13 716 | 89.53 | 18 963 | 96.80 | 18 623 | 98.47 |
| | 1.20 | 14 842 | 88.67 | 19 321 | 94.86 | 19 026 | 96.28 |
| Conv. Opt. (CO) | | 131 000 | | 18 376 | | 18 343 | |

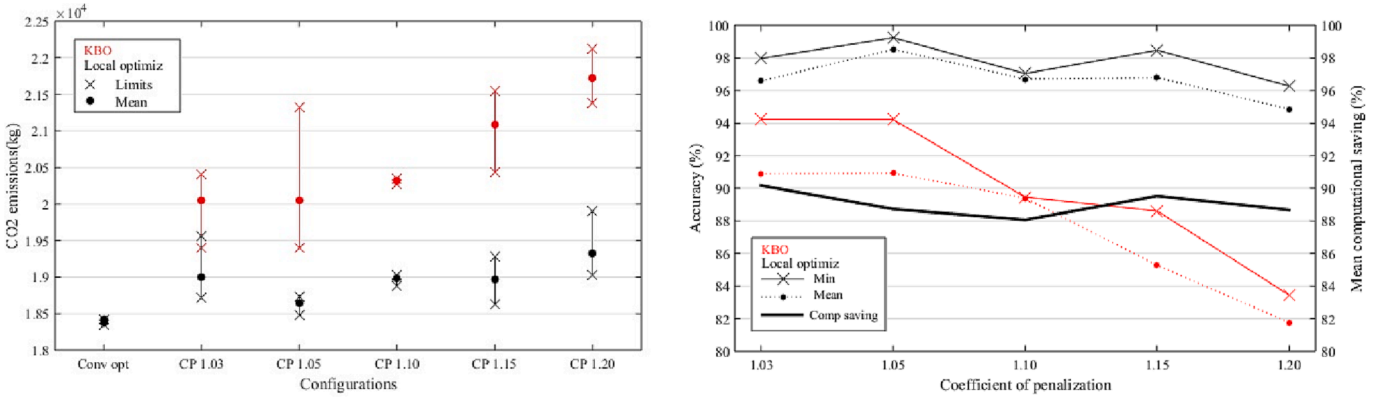


**Fig. 14.** Graphic comparison of results shown in Table 8. Left: simple box plots (extreme values and mean) of three test performed for each configuration. Right: Accuracy of metamodel-based optimization results (in comparison to CO) for different CPs (left y-axis) and corresponding computational savings (right y-axis).

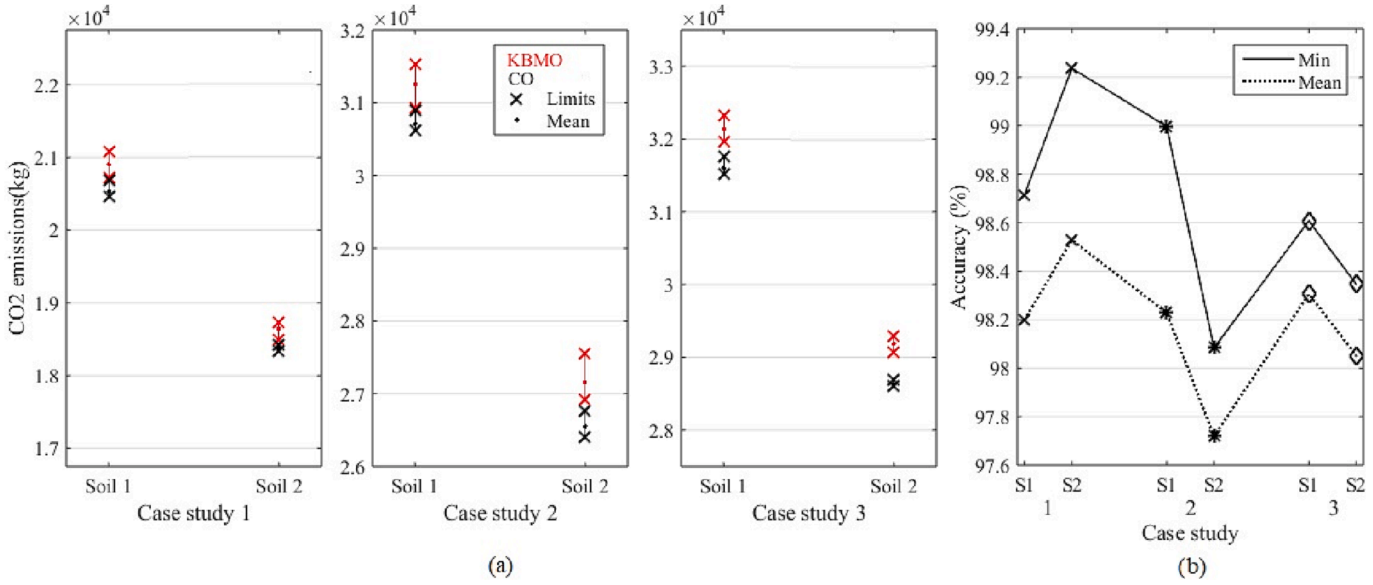


**Fig. 15.** (a) Simple box plots of the three tests performed (conventional optimization and KBMO) for each case study for both soil types. (b) Achieved accuracy of KBMO compared to CO for each case. Note that the differences between the means and the minimum value obtained from the three tests are represented.

shows that the model for structure 2 is the most difficult to optimize, especially for soil 2, as shown in part (b). It is because this structure is probably more prone to obtain infeasible solutions. In this case, as the length of the beams increases, this infeasibility is given by the stiffness constraint of these elements (i.e., violation of the deflection constraint at the center of the span). This situation, as mentioned, becomes more critical in soil 2, causing a more stressed superstructure. This theory about the inversely proportional relationship between the number of infeasible solutions and the accuracy of metamodel-assisted optimization strategies is verified by obtaining less accurate results for case studies 2 and 3. Additionally, this is proven by the fact that the structures modeled on soil 2 are more challenging to optimize using the metamodel strategy. In Fig. 15(b), the results for model 1 suggest the opposite, but this is true for this case of CP = 1.05 specifically. In the previous section, it was found that, in general, the results are more stable for soil 1.

In summary, it can be stated that the results are pretty satisfactory since, on average, solutions above 98% accuracy are achieved compared to conventional optimization. In some specific cases, even 99% is exceeded. Regarding computational savings, a similar analysis is performed for CS-2 and 3 as for CS-1 (tables 7 and 8). For CS-2, these savings, on average, are 90% and 89 % for soils 1 and 2, respectively. For CS-3, the results are slightly higher: 90.5 and 89.4 %. In general, these results are similar to those obtained in CS-1.

### 3.2.3. *Exploring the systems under investigation*

One of the benefits of using metamodels is that thanks to the cheapness of the simulations, several experiments can be performed, and the solution space can be explored better. It allows a deeper understanding of the systems under analysis. Considering that several solutions were obtained in the study of the appropriate CP using CS-1, these are used to go inside into the structure's behavior. Other more generalized conclusions are also accepted by analyzing the solutions obtained with the other two case studies.

Hypotheses on the behavior of this type of structure, such as obtaining more stressed superstructures when modeling the SSI, have been previously discussed. Several of these hypotheses can be deduced from Fig. 16. Perhaps the most notable case is the relationship between the cost of beams and columns. It is often the case that as the cost of concrete in beams decreases, there is an increase in the cost of columns, significantly reinforcing steel, as can be seen in Fig. 16(c) comparing the cases of CP=1.05 with CO or with CP=1.10. The same occurs in Fig. 16 (d) with CP=1.03 compared to CP=1.05 or CP=1.10 with CP=1.15. It is because stiffer (more expensive) beams cause the columns to be

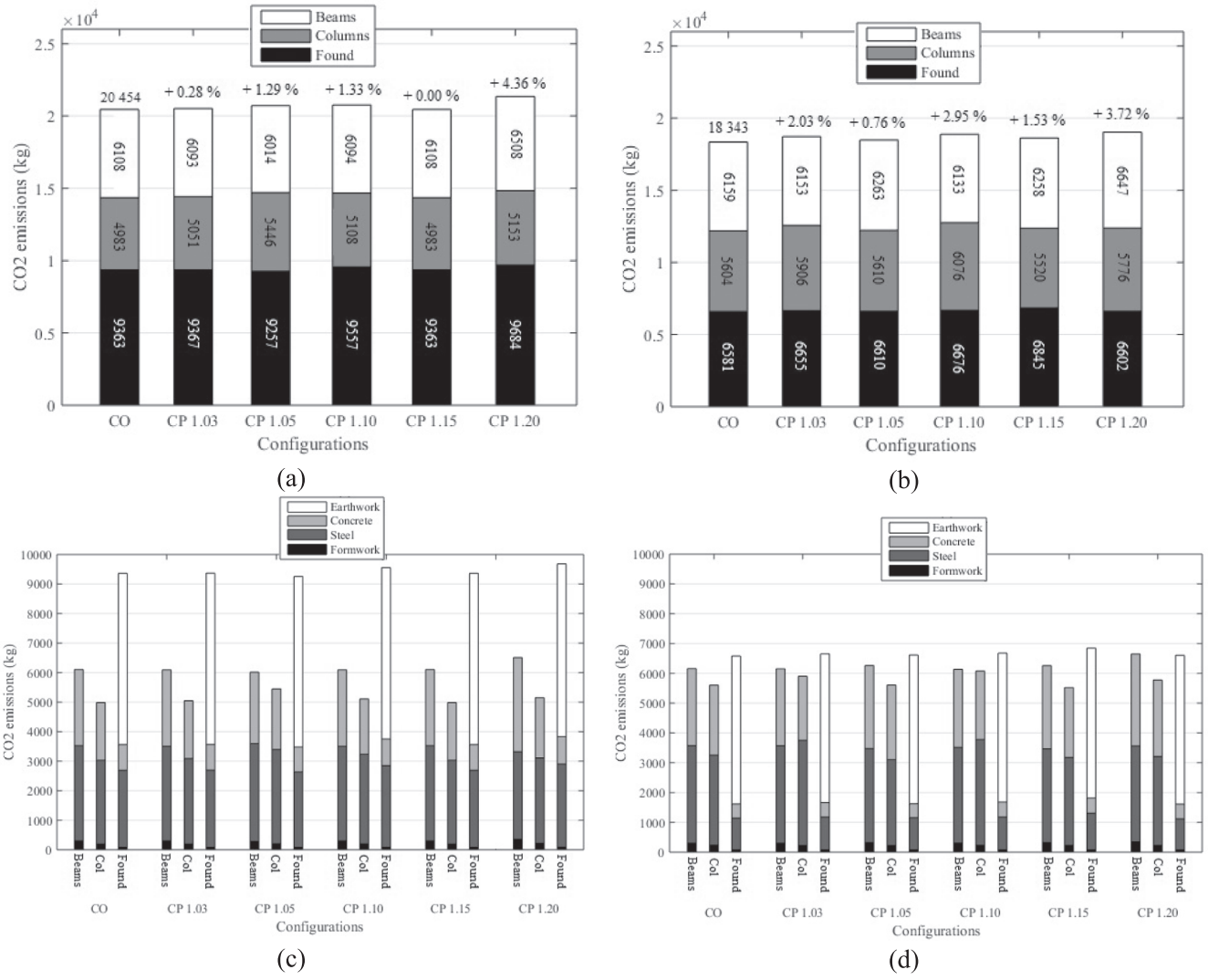


**Fig. 16.** Breakdown of each of the best solutions obtained by each configuration for CS-1, (a) and (b) represent the emissions broken down by elements, while (c) and (d) denote each element broken down by the main components. Additionally, (a) and (c) are related to the soil 1, while (b) and (d) to the soil 2.

subjected to fewer bending moment and a corresponding reduction in reinforcing steel.

It is essential to note the differences between the solutions for each soil type. Fig. 16(a) and (b) show that the columns of models with soil 2 are more expensive, although the foundations are much cheaper due to the higher bearing capacity of this type of soil. Considering that foundations are usually ignored in this type of study, a few lines are dedicated to their influence on the structural assembly. In CS-1, foundations represent 46 and 36% of the emissions of the structural assembly for soils 1 and 2, respectively. In CS-2, they represent 41 and 29 %, while in CS-3, 40 and 26 %, respectively. Therefore, foundations are very influential in the final output of this type of structure. In addition, they regulate how the superstructure works with their geometry and the interaction with the soil. It is also essential to emphasize the significant impact on $CO_2$ emissions of earthwork activities. In CS-1, they represent 62% of the total emissions of foundations (28% of global emissions) for soil 1 and 75% (27% of the total) for soil 2. In CS-2, this ratio is 51% (21% of the total) for soil 1 and 69% (20% of the total) for soil 2. For CS-3, these values are 51% (20%) and 71% (18%), respectively.

Other significant aspects are the optimal emission ratios between elements and components. For CS-1 with soil 1, the distribution is approximately 30, 24, and 46% between beams, columns, and foundations. In the case of soil 2, this distribution is more equitable, leaving 33, 31, and 36%. For CS-2, this distribution is 34–25-41 for soil 1 and 40–31-29 for soil 2. In CS-3, the optimal distribution would be 32–28-40 for soil 1 and 36–38-26 for soil 2. Regarding the components analyzed, it can be seen that the formwork has very little influence, unlike the earthwork. On the other hand, the optimal (environmental) cost ratio of steel–concrete is always helpful in reinforced concrete structures. For the CS-1 with soil 1, this ratio is 1.25, 1.45, and 3.01 for beams, columns, and foundations, respectively. For soil 2, the ratios are 1.25, 1.29, and 2.23. The overall ratios are 1.61 for soil 1 and 1.37 for soil 2. For the second case study, these ratios are 1.08, 1.57, and 3.47 (1.60 in general) for soil 1, and 0.96, 1.31, and 2.42 (1.20 in general) for soil 2. CS-3′s optimal distribution is 1.12, 1.20, and 3.39 (1.47 in general) for soil 1, and 1.05, 1.51, and 2.35 (1.33 in general) for soil 2.

## 4. Concluding remarks and future work

Although conventional heuristic optimization has been successfully implemented for years in structural optimization, this strategy may be insufficient to deal with more complex problems. This increase in complexity is due to the development of more accurate models, even though modeling aspects such as soil-structure interaction (SSI) are usually not considered. This paper has evaluated the use of metamodel-assisted optimization to minimize the $CO_2$ emissions of spatial

reinforced concrete frame buildings, taking into account the SSI, which is implemented using a Winkler model. The surrogate models are built using a Kriging-based methodology.

Due to the particularities of the formulated discrete optimization problem, there are better alternatives than simple Kriging-based optimization. Thus, a meta-heuristic strategy is proposed using a Kriging-based two-phase methodology to build the surrogate model with a local search algorithm.

Results show that the SSI should be addressed during modeling. When considering this aspect, the superstructure design provides different results than when it is not considered, i.e., the SSI consideration leads to more stressed superstructures, especially the columns. This phenomenon is more evident in predominantly frictional soils than in predominantly cohesive ones. Considering the foundations within the structural assembly is another aspect that should be addressed. They are very influential both in the general outputs of the structure and in the way in which the system distributes the loads. On the other hand, applying the Kriging-based meta-heuristic optimization allows for obtaining very accurate results compared with those obtained with the conventional heuristic optimization, with computational savings of about 90%. This accuracy varies depending on the coefficient of penalization. Generally, better results are obtained for low coefficients (1.03–1.05).

Promising lines of research in this field should focus on implementing surrogate-based optimization to solve optimization problems with more encompassing formulations, considering environmental, social, and constructive objectives. Moreover, these objectives should not only be limited to mere optimization up to the design stage, i.e., they should also include the Life-Cycle Analysis of the structures. Another interesting point of view would be identifying the least influential variables within the optimization results and converting them into constant parameters by assigning them values that have proven optimal from previous studies. It would make the optimization problem easier to solve, considerably reducing computation time. Alternatively, considering that soil-structure interaction is a novel aspect in this research, the influence of soil conditions underlying the foundations, such as the presence of a water table, more than one stratum, or drainage conditions, could be investigated. Other ways of modeling this interaction can also be explored. An interesting alternative would be implementing other models beyond the proposed linear springs, such as using dashpots with a Kelvin-type or a similar approach. It would be very effective also for dynamic analysis. Therefore, further refining the proposed methodology with other more complex methods and checking if it is worthwhile would be fascinating. In addition, other artificial intelligence techniques (e.g., Neural Networks) could be considered to deal with the high computational costs. Furthermore, once the importance of modeling SSI in frame structures has been demonstrated, other typologies should be tested to increase the sustainability of this type of structure based on the methodologies proposed in this work. Once more complex structures are implemented, other foundation alternatives such as combined footings, mat foundations, or mat-piles combinations can be used. An exciting research to develop would be to analyze the sustainability of each of them and their relation with the superstructure design. Regarding the latter, variable section beams, “I” or “T” sections, slab-column typologies (without beams), hybrid elements, and others can be alternatives to be explored to improve the economic, environmental, constructive, social, and durability indexes of this type of construction. Another promising line of research is focused on the type of optimization formulation. Performance-based, reliability-based, or robust designs are interesting and efficient approaches when considering other aspects, such as dynamic analysis or uncertainty.

## CRediT authorship contribution statement

**Iván Negrin:** Conceptualization, Methodology, Software, Investigation, Formal analysis, Visualization, Writing – original draft. **Moacir Kripka:** Conceptualization, Writing – review & editing, Supervision, Project administration. **Víctor Yepes:** Conceptualization, Resources, Supervision, Project administration, Writing – review & editing, Funding acquisition.

## Declaration of Competing Interest

The authors declare that they have no known competing financial interests or personal relationships that could have appeared to influence the work reported in this paper.

## Data availability

Data will be made available on request.

## Acknowledgments

This work was supported by the grant PID2020-117056RB-I00, which was funded by MCIN/AEI/10.13039/501100011033 and by “ERDF A way of making Europe”. Grant PRE2021-097197 funded by MCIN/AEI/10.13039/501100011033 and by FSE+.

## References

[1] Negrin I, Roose D, Chagoyén E, Lombaert G. Biogeography-Based Optimization of RC structures including static soil structure interaction. Struct Eng Mech 2021;80(3):285–300. https://doi.org/10.12989/sem.2021.80.3.285.
[2] Gartner E. Industrially interesting approaches to “low-$CO_2$ cements”. Cem Concr Res 2004;34(9):1489–98. https://doi.org/10.1016/j.cemconres.2004.01.021.
[3] Thormark C. A low energy building in a life cycle-its embodied energy, energy need for operation, and recycling potential. Build Environ 2002;37(4):429–35. https://doi.org/10.1016/S0360-1323(01)00033-6.
[4] Yeo D, Gabbai R. Sustainable design of reinforced concrete structures through embodied energy optimization. Energ Buildings 2001;43(8):2028–33. https://doi.org/10.1016/j.enbuild.2011.04.014.
[5] Penadés-Plà V, García-Segura T, Yepes V. Accelerated optimization method for low-embodied energy concrete boxgirder bridge design. Eng Struct 2019;179:556–65. https://doi.org/10.1016/j.engstruct.2018.11.015.
[6] Camp CV, Huq F. CO2 and cost optimization of reinforced concrete frames using a big bang-big crunch algorithm. Eng Struct 2013;48:363–72. https://doi.org/10.1016/j.engstruct.2012.09.004.
[7] Yepes V, Martí JV, García-Segura T. Cost and CO2 emission optimization of precastprestressed concrete U-beam road bridges by a hybrid glowworm swarm algorithm. Autom Constr 2015;49:123–34. https://doi.org/10.1016/j.autcon.2014.10.013.
[8] Negrin IA, Chagoyén E. Economic and environmental design optimisation of reinforced concrete frame buildings: A comparative study. Structures 2022;38:64–75. https://doi.org/10.1016/j.istruc.2022.01.090.
[9] Paya I, Yepes V, González-Vidosa F, Hospitaler A. On the Weibull cost estimation of building frames designed by simulated annealing. Meccanica 2010;45:693–704. https://doi.org/10.1007/s11012-010-9285-0.
[10] Molina-Moreno F, García-Segura T, Martí JV, Yepes V. Optimization of buttressed earth-retaining walls using hybrid harmony search algorithms. Eng Struct 2017;134:205–16. https://doi.org/10.1016/j.engstruct.2016.12.042.
[11] Kaveh A. Advances in Metaheuristic Algorithms for Optimal Design of Structures, Springer International Publishing, Switzerland, 3rd edition, 2021. 10.1007/978-3-319-05549-7.
[12] Kaveh A. Applications of Metaheuristic Optimization Algorithms in Civil Engineering, Springer. Switzerland 2017. https://doi.org/10.1007/978-3-319-48012-1.
[13] Olivier J, Janssens-Maenhout G, Muntean M, Peters J, Trends in Global CO2 Emissions,. Report. Joint Research Centre, Hague: European Commission; 2015.
[14] Lagaros N. A general purpose real-world structural design optimization computing platform. Struct Multidiscip Optim 2013. https://doi.org/10.1007/s00158-013-1027-1.
[15] Esfandiari M, Urgessa G, Sheikholarefin S, Dehghan Manshadi G. Optimum design of 3D reinforced concrete frames using DMPSO algorithm. Adv in Eng Soft 2018;115:149–60. https://doi.org/10.1016/j.advengsoft.2017.09.007.
[16] Martins A, Simões L, Negrão J, Lopes A. Sensitivity analysis and optimum design of reinforced concrete frames according to Eurocode 2. Eng Opt 2019. https://doi.org/10.1080/0305215X.2019.1693554.
[17] Mergos P. Optimum design of 3D reinforced concrete building frames with the flower pollination algorithm. J Build Eng 2021;44. https://doi.org/10.1016/j.jobe.2021.102935.
[18] Salimi P, Bondarabadi H, Kaveh A. Optimal Design of Reinforced Concrete Frame Structures Using Cascade Optimization Method. Period Polytech-Civ Eng 2022;66(4):1220–33. https://doi.org/10.3311/PPci.20868.

[19] Filomeno-Coelho R. Metamodels for mixed variables based on moving least squares. Application to the structural analysis of a rigid frame. Optim Eng 2013. https://doi.org/10.1007/s11081-013-9216-8.

[20] Bäckryd RD, Ryberg AB, Nilsson L. Multidisciplinary design optimisation methods for automotive structures. Int. J. Automot. Mech. Eng., 2017, 14(1), pp. 4050-67. 10.15282/ijame.14.1.2017.17.0327.

[21] Negrin I, Chagoyén E, Negrin A. Parameter tuning in the process of optimization of reinforced concrete structures. DYNA 2021;88(216):87–95. http://doi.org/10.15446/dyna.v88n216.87169.

[22] Navarro I, Yepes V, Martí JV, González-Vidosa F. Life cycle impact assessment of corrosion preventive designs applied to prestressed concrete bridge decks. J Clean Prod 2018;196:698–713. https://doi.org/10.1016/j.jclepro.2018.06.110.

[23] Pons JJ, Penadés-Plà V, Yepes V, Martí JV. Life cycle assessment of earth-retaining walls: An environmental comparison. J Clean Prod 2018;192:411–20. https://doi.org/10.1016/j.jclepro.2018.04.268.

[24] Khatibinia M, Salajegheh E, Salajegheh J, Fadaee M. Reliability based design optimization of reinforced concrete structures including soil structure interaction using a discrete gravitational search algorithm and a proposed metamodel. Eng Optim 2013;45(10):1147–65. https://doi.org/10.1080/0305215X.2012.725051.

[25] Zhang Y, et al. Two-dimensional nonlinear earthquake response analysis of a bridge-foundation-ground system. Earthq Spectra 2018;24:343–86. https://doi.org/10.1193/1.2923925.

[26] Klepikov SN. General solution for beams and plates on elastically deforming bases with varying stiffnesses. In: Bases, foundations and soil mechanics research. Budivielnik: Kiev; 1969. p. 37–47.

[27] Klepikov SN, Tregub AS, Matveev IV. Calculation of buildings and works on collapsible soils. Kiev: Budivielnik; 1987.

[28] Bao T, Lui Z. Evaluation of Winkler Model and Pasternak Model for Dynamic Soil-Structure Interaction Analysis of Structures Partially Embedded in Soils. Int. J. Geomech., Vol. 20, No. 2. 10.1061/(ASCE)GM.1943-5622.0001519.

[29] Matlock, H. Correlations for design of laterally loaded piles in soft clay. In Vol. 1204 of Proc., Offshore Technology in Civil Engineering's Hall of Fame Papers from the Early Years, 1970, 77–94. Houston: Offshore Technology Conference. 10.4043/1204-ms.

[30] Cox W., Reese L. C., Grubbs B. R. Field testing of laterally loaded piles in sand. In Proc., Offshore Technology Conf., 1974, 1–14. Houston: Offshore Technology Conference. 10.4043/2079-MS.

[31] Reese LC, Welch RC. Lateral loading of deep foundations in stiff clay. J Geotech Eng Div 1975;101(7):633–49. https://doi.org/10.1061/AJGEB6.0000177.

[32] Taghavi A, Muraleetharan KK. Analysis of laterally loaded pile groups in improved soft clay". Int J Geomech 2016;17(4):1–13. https://doi.org/10.1061/(ASCE)GM.1943-5622.0000795.

[33] Mottaghi L, Izadifard RA, Kaveh A. Factors in the Relationship Between Optimal $CO_2$ Emission and Optimal Cost of the RC Frames. Period Polytech-Civ Eng 2021;65(1):1–14. https://doi.org/10.3311/PPci.16790.

[34] Kaveh A, Izadifard RA, Mottaghi L. Optimal design of planar RC frames considering CO2 emissions using ECBO, EVPS and PSO metaheuristic algorithms. J Build Eng 2020;28. https://doi.org/10.1016/j.jobe.2019.101014.

[35] Kaveh A. Cost and $CO_2$ Emission Optimization of Reinforced Concrete Frames Using Enhanced Colliding Bodies Optimization Algorithm. In: Applications of Metaheuristic Optimization Algorithms in Civil Engineering. Cham: Springer; 2017. https://doi.org/10.1007/978-3-319-48012-1_17.

[36] Catalonia Institute of Construction Technology. BEDEC PR/PCT ITEC material database; 2016.

[37] Medeiros GF, Kripka M. Optimization of reinforced concrete columns according to different environmental impact assessment parameters. Eng Struct 2014;59:185–94. https://doi.org/10.1016/j.engstruct.2013.10.045.

[38] Medeiros GF, Kripka M. Modified harmony search and its application to cost minimization of RC columns. Adv. Comput. Des., 2017, 2(1), pp. 1-13. 10.12989/acd.2017.2.1.001.

[39] Yepes V, García-Segura T, Martí JV, Alcalá J. Optimization of concrete I-beams using a new hybrid glowworm swarm algorithm. Lat Am J Solids Struct 2014;Volumen 11:1190–205. https://doi.org/10.1590/S1679-78252014000700007.

[40] Serpik I, Mironenko I, Averchenkov V. Algorithm for Evolutionary Optimization of Reinforced Concrete Frames Subject to Nonlinear Material Deformation-International Conference on Industrial Engineering, ICIE 2016. Procedia Engineering, Issue 150, pp. 1311-16. 10.1016/j.proeng.2016.07.304.

[41] Negrin I, Negrin MA, Chagoyén E. Optimización de pórticos planos de hormigón armado utilizando una hibridación de algoritmos genéticos y el algoritmo Nelder-Mead. Obras y Proyectos 2019;26:74–86. https://doi.org/10.4067/S0718-28132019000200074.

[42] Triches-Boscardin J, Yepes V, Kripka M. Optimization of reinforced concrete building frames with automated grouping of columns. Autom Constr 2019;104:331–40. https://doi.org/10.1016/j.autcon.2019.04.024.

[43] Paya I, Yepes V, Hospitaler A, González-Vidosa F. CO2-optimization of reinforced concrete frames by simulated annealing. Eng Struct 2009;31:1501–2158. https://doi.org/10.1016/j.engstruct.2009.02.034.

[44] García-Segura T, Penadés-Plá V, Yepes V. Sustainable bridge design by metamodel-assisted multi-objective optimization and decision-making under uncertainty. J Clean Prod 2018;202:904–15. https://doi.org/10.1016/j.jclepro.2018.08.177.

[45] Penadés-Plà V, Yepes V, García-Segura T. Robust decision-making design for sustainable pedestrian concrete bridges. Eng Struct 2020. https://doi.org/10.1016/j.engstruct.2019.109968.

[46] Mathern A, Penadés Plà V, Armesto-Barros J, Yepes V. Practical metamodel-assisted multi-objective design optimization for improved sustainability and buildability of wind turbine foundations. Struct Multidisc Optim 2022. https://doi.org/10.1007/s00158-021-03154-0.

[47] Martínez-Martín FJ, Yepes V, González-Vidosa F, Hospitaler A. Optimization Design of RC Elevated Water Tanks under Seismic Loads. Appl Sci 2022;12(5635). https://doi.org/10.3390/app12115635.

[48] Simon D. Biogeography-Based Optimization. IEEE Transactions on evolutionary computation, 2008, 12(6.), pp. 702-13. 10.1109.

[49] Aydogdu I. Cost optimization of reinforced concrete cantilever retaining walls under sismic loading using a boiogeograpy-based optimization algorithm with Levy flights. Eng Opt 2017;49(3):381–400. https://doi.org/10.1080/0305215X.2016.1191837.

[50] Shallan O, Maaly HM, Sagiroglu M, Hamdy O. Design optimization of semi-rigid space steel frames with semi-rigid bases using biogeography-based optimization and genetic algorithms. Struct. Eng. Mech., 2019, 70(2), pp. 221-31. 10.12989/sem.2019.70.2.221.

[51] Negrin I, Roose D, Chagoyén E. Parameter tuning strategies for metaheuristic methods applied to discrete optimization of structural design. Available at: Revista Inv Op 2022;43(2):241–58. https://rev-inv-ope.pantheonsorbonne.fr/sites/default/files/inline-files/43222-08.pdf.

[52] Myers R, Montgomery D, Anderson-Cook C. Response surface methodology: process and product optimization using designed experiments 1995. https://doi.org/10.2307/1270613.

[53] Chuang CH, et al. Multidisciplinary design optimization on vehicle tailor rolled blank design. Struct Multidiscip Opt 2008;31:551–60. https://doi.org/10.1007/s00158-007-0152-0.

[54] McKay M, Beckman RJ, Conover WJ. Comparison of Three Methods for Selecting Values of Input Variables in the Analysis of Output from a Computer Code. Technometrics 1979;21(2):239–45. https://doi.org/10.1080/00401706.1979.10489755.

[55] Forrester AIJ, Keane AJ. Recent advances in surrogate-based optimization. Prog Aerosp Sci 2009;45:50–79. https://doi.org/10.1016/J.PAEROSCI.2008.11.001.

[56] Li YF, Ng SH, Xie M, Goh TN. A systematic comparison of metamodeling techniques for simulation optimization in decision support systems. Appl Soft Comput 2010;10:1257–73. https://doi.org/10.1016/J.ASOC.2009.11.034.

[57] Lophaven SN, Nielsen HB, Søndergaard J. DACE: A Matlab Kriging toolbox. Version 2.0., Kongens Lyngby, Denmark: Informatics and Mathematical Modelling, Technical University of Denmark, 2002. 10.2307/1270613.

[58] Krige DG. A statistical approach to some mine valuation and allied problems on the Witwatersrand. University of the Witwatersrand, South Africa; 1951. Master's thesis,Available at:.

[59] Cressie NAC. Statistics for spatial data. New York, NY, USA: John Wiley & Sons; 1993.

[60] Lophaven SN, Nielsen HB, Søndergaard J. Aspects of the Matlab toolbox DACE, Kongens Lyngby. Denmark: Informatics and Mathematical Modelling, Technical University of Denmark; 2002. Available at: https://citeseerx.ist.psu.edu/viewdoc/download?doi=10.1.1.69.7029&rep=rep1&type=pdf.

[61] Nelder JA, Mead R. A simplex method for function minimization. Comput J 1965;7:308–13. https://doi.org/10.1093/comjnl/7.4.308.

[62] Dantzig GB. Linear Programming and Extensions. Santa Monica, California: Princeton University Press, 1963. Dantzig GB. Linear Programming and Extensions. Santa Monica, California: Princeton University Press, 1963. 10.7249/R366.